Possible Futures in Sight: Disability Service Facilities and Local Fertility*

Atsushi Yamagishi†

September 11, 2026
Very Preliminary

Abstract

This paper examines whether incidental social contact with people with disabilities and their caregivers influences fertility decisions by making perceived disability risk and anticipated care needs more salient. Using spatially-granular census data in Japan, I find 7.39 fewer children ages 0–4 per 1,000 women ages 15–49, about 3.9% of the mean child-to-woman ratio, near the disability service facility. Furthermore, child–woman ratios are lower along the path between the facility and public transportation points and the proximity to the facility has a larger impact stronger where private-car use is lower. Placebos based on facilities' entry timing and elderly care facilities do not reproduce lower child-to-woman ratio. Adjustments for residential sorting, land prices, and safety level leave most of the association in place. These patterns imply that more opportunities for incidental encouters with people with disability and their caregivers in a neighorhood may affect the anticipated disability risk or care needs, thereby affecting fertility decisions.

Keywords: fertility decisions; disability; risk perceptions; incidental social contact; neighborhood effects

JEL codes: I10, J13, I14, R23, Z13

*Yamagishi appreciates the financial support from JSPS KAKENHI Grant Numbers 25K00629, 26K22083, 26K00327m and 24H00150. All remaining errors are mine.
†Institute of Economic Research, Hitotsubashi University & IZA. E-mail: atsushiyamagishi.econ@gmail.com.

1 Introduction

Amid the global decline in fertility, understanding what shapes decisions about whether and when to have children is increasingly important (Doepke et al., 2023; Kearney and Levine, 2026). An important consideration in these decisions is uncertainty about the future demands of parenthood, given that having a child is an irreversible decision (de la Croix and Pommeret, 2021). In particular, childhood disability can entail substantial caregiving demands and adversely affect parents' employment and mental health (Cheung et al., 2025; Asuman et al., 2025; Chen et al., 2026), and anticipating these consequences may discourage childbearing even before a child is conceived. Fertility decisions may therefore depend on how people perceive both the likelihood of having a child with a disability and the care needs and costs they might face.

This paper examines this possibility using disability service facilities in Japan, whose experience of below-replacement fertility since the mid-1970s makes it a particularly informative setting (OECD, 2024). These facilities may increase opportunities to see adults with disabilities and accompanying caregivers in everyday public spaces. These brief encounters, which I refer to as *incidental social contact*, can make disability and potential lifelong care needs more salient, potentially increasing the perceived likelihood of having a child with a disability or the anticipated costs of raising one. I examine whether fertility rates are lower near these facilities and whether this negative association is stronger where prospective mothers are more likely to encounter adults with disabilities and their caregivers.

I begin by testing whether fertility rates are lower in areas closer to the disability service facilities, which would provide more opportunities for the incidental social contact. I use Japan's 2020 Population Census to define the child–woman ratio (CWR), the number of children ages 0–4 per 1,000 women ages 15–49. Measured in 250 m grid cells, the CWR, a common proxy of fertility, permits comparisons over distances of a few city blocks. Combining this local measures of the fertility with geocoded facilities from the 2021 National Land Numerical Information Welfare Facilities Data, I estimate distance-band profiles within 1.5 km of the nearest facility. The preferred specification includes additive nearest-facility and parent-500 m fixed effects and ten demographic, zoning, and housing controls, making sure to compare similar areas that differ only in the exposure to the disability service facilities. The baseline specification shows 7.39 fewer children ages 0–4 per 1,000 women ages 15–49 within 250 m of a facility than at 1.25–1.50 km. This difference is statistically significant at the 5 percent level and is equivalent to 3.9 percent of the weighted sample mean. The next two distance bands show similar negative differences, while those beyond 750 m are smaller and statistically indistinguishable from zero.

I then provide two additional pieces of evidence suggesting that the lower fertility around the disability service facilities likely stems from more opportunities for incidental social contact. First, social contact would be more likely to arise on walking routes from facilities to their nearest stations and bus stops, along which residents may encounter facility users and caregivers. In contrast, less opportunities for the incidental social contact would arise on "placebo" routes that connects the facility with hypothetical train or bus stops. Consistent with this hypothesis, I find that the coefficient on the actual-path indicator is 3.42 CWR points lower than the average coefficient on three placebo-path indicators constructed by rotating the transit destinations. Second, I test how the lower fertility rate around the disability service facilities interacts with the car usage rate, motivated by the idea that private-car travel may reduce opportunities for encounters on neighborhood streets. I find that the estimated CWR difference between cells within 250 m of a facility and those 1.25–1.50 km away is −19.28 at the 10th percentile of local car use (8.5 percent), compared with 0.26 at the 90th percentile (79.1 percent). The 19.53-point contrast suggests a stronger negative proximity association where car use is lower. The car-use evidence is therefore suggestive of the importance of the incidental social contact in the city.

I conduct a bunch of analyses to assess the role of other explanations behind the lower CWR around the disability service facilities. I begin by conducting two placebo tests to assess the possibility that the lower fertility around the disability service facility captures some unobserved local characteristics, rather than the effect of the facility. In the first placebo test, I find that the 2015 CWR was not significantly lower around candidate future facilities observed in 2021 after screening out nearby or text-matched welfare facilities in both the 2011 and 2015 records. This provides no evidence of a comparable negative pre-existing CWR gradient around these candidate locations. In the second placebo test, I find that no lower CWR is observed around elderly care facilities, which primarily address care needs associated with aging. In addition, I also explicitly examine three alternative explanations behind the lower CWR: migration, land price, and safety. First, although the CWR is biased downward if familites with more children tend to move out on net, controlling for the local net migration rates of children only modestly attenuates the lower CWR estimate around the disability service facilities. Land prices and safety levels could also respond to the presence of the disability service facilities while directly affecting the fertility decisions, but conditioning on measured land prices or theft rates retains the lower CWR. Overall, I find that alternative explanations play, at most, a limited role in explaining the lower CWR around the disability service facilities, leaving the incidental social contacts lowering fertility rates as the primary explanation.

These patterns suggest that anticipated caregiving demands and uncertainty about available support may enter fertility decisions. These findings motivate further research on disability-related expectations and access to reliable information and support. These findings also suggest a potential *ex ante* insurance value of public disability support. If concerns about future caregiving demands discourage childbearing, confidence that financial assistance and care services will be available when needed could reduce the burdens and uncertainty prospective parents expect to face. This reassurance could benefit people who never ultimately use these services, leading to a higher fertility rate. For example, Einav et al. (2025) highlights that the economic cost of having a child with a disability in Sweden could be small under its generous welfare system. Such a generous welfare system for familites with a child with a disability certainly helps them, but it may also benefit the entire families beyond them as an insurance and lead to a higher fertility rate.

This paper relates to several strands of literature. First, the paper relates to evidence that reproductive behavior responds to risks to a child's health and to information about those risks. For example, research on the Zika epidemic documents reductions in pregnancies and births following public information linking infection during pregnancy to microcephaly and other congenital conditions (Lautharte and Rasul, 2026; Rangel et al., 2020). Evidence from Japan's rubella epidemic and from reproductive responses after Chernobyl likewise links fertility timing to concerns about fetal health (Mizumoto and Chowell, 2020; Bertollini et al., 1990). These studies highlight both health hazards and the information through which households perceive them. Avoiding fertility during the epidemics relating to the congenital disability is consistent with the complementary literature documenting the economic and welfare costs of raising children with disabilities (Chen et al., 2026; Cheung et al., 2025; Asuman et al., 2025; Frijters et al., 2009; Skoy, 2024).[1] I extend this perspective to everyday neighborhood exposure outside a public-health crisis. Indeed, a nearby disability facility does not raise the biological probability of having a child with a disability, but it may make that possibility and anticipated caregiving needs more salient, highlighting the role of the *perceived* risk of having a child with a disability.

Second, more broadly, this paper relates to the determinants of fertility. The standard economics approach views childbearing as a household's utility maximization behavior, influenced by income, the costs of raising children, and the allocation of resources between the number of children and investment in each child (Becker, 1960; Becker and Lewis, 1973). In addition to the role of income (Black et al., 2013), recent work emphasizes the compatibility of careers and family life, including childcare provision, family policy, fathers' participation in care, social norms, and flexible labor markets (Doepke et al., 2023; Fernández et al., 2026).[2] Information also matters: experimentally provided information about maternal health risks changes subsequent pregnancy outcomes (Ashraf et al., 2026), while correcting beliefs about pregnancy probabilities changes stated contraceptive intentions (Miller et al., 2025). I bring disability-related expectations into this discussion by examining whether local opportunities for incidental encounters with people with disability are associated with differences in local fertility rates. Such encounters may make anticipated caregiving demands and uncertainty about available support more salient.

Finally, the paper relates to research on how social contact and information shape people's belief and behavior toward another social group. Contact theory raises the possibility that superficial encounters, such as seeing someone on a neighborhood street, leave existing stereotypes unchallenged or reinforce them (Allport, 1954). Although intergroup contact generally reduces prejudice, its effects depend on the form and quality of interaction (Pettigrew and Tropp, 2006; Lowe, 2021). In the present setting, incidental encounters may make anticipated care needs more salient, while sustained contact could increase familiarity and reduce concern. Local-

[1] These effects need not be uniformly large or negative , depending on the generosity of the welfare system (Einav et al., 2025). However, I expect the Japanese system is closer to the less-generous welfare system, such as the case of Taiwan (Cheung et al., 2025; Chen et al., 2026).

[2] The economics literature of fertility rates in Japan includes Hashimoto (1974), Yamaguchi (2019), Fukai and Toriyabe (2025), Kitao and Nakakuni (2026), and Kondo (2026).

interaction models about reproductive behavior provide a related account of how encounters shape beliefs and affect the fertility rate. In Munshi and Myaux (2006), individuals update beliefs about their community's reproductive norms from the actions of the people they meet, so different histories of encounters generate different beliefs and contraceptive choices. Kohler (2000) similarly shows how social networks can shape the transition toward lower fertility. Empirically, a fertility decision spreads among friends (Balbo and Barban, 2014) and that media portrayals of teenage parenthood might affect teen births (Kearney and Levine, 2015) further connects social exposure to reproductive behavior.[3] I study neighborhood differences in opportunities for incidental encounters with people with disability and their caregivers as one such source of exposure.

The rest of the paper is organized as follows. Section 2 introduces my empirical hypotheses while presenting illustrative qualitative accounts. Section 3 describes the data, sample construction, and empirical design. Section 4 presents my main results about the disability service facility and the fertility, provides additional evidence that the incidental social contact seems important, and assesses alternative explanations through placebo analyses and explicitly accounting for migration, land prices, and safety concerns. Section 5 presents robustness checks. Section 6 concludes. Online Appendix provides further details on the data construction, empirical specifications, and supplementary results.

2 Hypotheses and Qualitative Motivation

A disability service facility does not change the biological probability that a nearby resident will have a child with a disability. Facilities may nevertheless concentrate opportunities for brief, incidental public encounters with service users and accompanying caregivers on nearby streets and along routes to rail stations or bus stops. At least for some observers, such indidental social contacts may make the possibility of raising a child with a disability and its perceived consequences easier to imagine.[4] This hypothesized salience could increase the subjective weight placed on anticipated long-term care, financial pressure, or effects on other family members when deciding whether or when to have a child.[5]

Qualitative accounts To provide suggestive qualitative accounts of this hypothesis, I conducted a purposive, non-systematic online search of publicly accessible Japanese-language discussion boards, question-and-answer sites, and edited first-person or interview-based web arti-

[3]See Jaeger et al. (2020) for a critical reassessment of Kearney and Levine (2015).

[4]Note that the anticipated contact is brief, and I acknowledge that a more sustained or favorable type of contact could instead reduce unfamiliarity and concern (Pettigrew and Tropp, 2006; Lowe, 2021). That said, the quoted responses in the social media below suggest that such interactions, such as working for a disability facility, may still increase the perceived cost of having a child with a disability and deter childbirth.

[5]The irreversible nature of childbearing decisions has the key role (de la Croix and Pommeret, 2021): If people can "cancel" having a children with disability, they do not need to care about their care needs. The irreversibility creates the insurance value of welfare system for helping people with disability and their caregivers, which I briefly mention again in the conclusion (Section 6).

cles to find opinions that are consistent with this hypothesis.[6] They illustrate that the proposed sequence can be articulated in at least some of individual accounts.[7] I quote the English translation of the exerpts below:[8]

- "The mothers I see accompanying people around town [...] when I think there is a chance I might have a child with an intellectual disability, I cannot have children."[9]
- "I also do not want to become the parent of a person with a disability [...] I often encountered children with disabilities through my work [...] I do not have the confidence to care for an adult with a disability."[10]
- "I sometimes see people accompanying children with profound disabilities [...] I am not confident that I could raise my own child if they were in that condition."[11]
- "I see people with Down syndrome at a disability facility [...] I absolutely could not give birth after such a diagnosis."[12]
- "My experience during the practicum, when I felt that I probably could not raise [a child with a disability], was also part of the background [to my decision to undergo prenatal testing]."[13]
- "Could I bear even some of the hardship [mothers raising children with disabilities] face?"[14]

Related themes also appear in independent peer-reviewed research. Takeda et al. (2025) analyze open-ended responses from 754 Japanese women undergoing noninvasive prenatal testing (NIPT), a maternal blood test that screens for certain fetal chromosomal conditions. Of these responses, 48.1 percent include negative thoughts about raising a child with special needs, and 22.3 percent discuss NIPT and life selection. In 333 English-language and 519 Mandarin-language pregnancy-forum responses, Li et al. (2017) likewise identify narratives linking disability and support to prenatal testing and abortion in the United States and mainland China. Together with the above excerpts, they reinforce the hypothesis that the anticipated probability

[6] To focus on contact outside the family, I excluded accounts in which the writer's own disability or a relative's disability was the principal source of concern.

[7] Although the accounts quoted here predominantly reflect women's perspectives, similar concerns may also shape men's reproductive choices. In her U.S. interview-based doctoral dissertation, Kissling (2020, pp. 37–38) describes Alvin, a 29-year-old childfree man, and links his observation of the care required by children with disabilities whom his mother cared for to his decision to seek a vasectomy. He explained, "I don't want to take that risk." The children's relationship to him is unspecified.

[8] Note that some wording is stigmatizing to keep the writer's original meanings: it does not represent an objective nor the author's characterization of the lives of people with disabilities or their families.

[9] GirlsChannel, comment 403, posted January 30, 2018 (accessed September 4, 2026).

[10] GirlsChannel, comment 112, replying to comment 83, posted July 23, 2017 (accessed September 4, 2026).

[11] Yahoo! Chiebukuro answer, posted March 18, 2026 (accessed September 4, 2026).

[12] Mamastar, comment 276, posted January 26, 2017 (accessed September 4, 2026).

[13] Mitsuko Tateishi, 「自閉症の息子妊娠中、出生前診断を受けた私」["During Pregnancy with My Autistic Son, I Underwent Prenatal Testing"], *LITALICO Hattatsu Navi*, published January 17, 2022 (accessed September 4, 2026).

[14] Miyuki Ono, 「出生前診断を受けた私が、本当に恐れていた『母の愛』への過剰な期待」["What I Really Feared When I Underwent Prenatal Testing"], *withnews*, published July 5, 2023 (accessed September 4, 2026).

or the care needs of having a child with a disability could be made more salient by the (incidental) social contact with people with disability and their caregivers.

Testable predictions. If the incidental social contact with people with disability and their caregivers raises the perceived risk or cost of having a child with a disability, it is natural to hypothesize that fertility should be lower in places with more opportunities for incidental encounters. Indeed, recent evidence using the GPS data has shown that a facility changes the number and the composition of the attracted people, shaping the pattern of social interactions (Atkin et al., 2022; Nilforoshan et al., 2023; Couture et al., 2025; Massenkoff and Wilmers, 2025). Motivated by this evidence that local facilities help structure opportunities for encounters, I hypothesize that the geographical proximity to the disability service facility, which attracts many people with disability and their caregivers, provides more opportunities to the incidental social contact:

Hypothesis 1 (facility proximity and fertility rates). Proximity to the nearest adult disability-service facility lowers the local fertility rate, with the largest effect in the immediate vicinity and attenuation over distance.

Note that in Hypothesis 1, the geographical proximity is just a proxy of the intensity of the incidental social contact. There are additional proxies of the social contact, which could further reduce the fertility rate. For example, if someone's residence is on a route between the facility and the nearest train or bus station, then they would have more opportunities of the incidental social contact because they are more likely to observe people with disability and their caregivers, who are travelling between the facility and the public transportation point, on the street. Another example is the local car usage rate. If the main mode of transportation is the private car, then observing people with disability and their caregivers on a street becomes more difficult, leading to limited opportunities of the incidental social contact. This leads to the following next hypothesis:

Hypothesis 2 (heterogeneity by opportunities for incidental social contact). The negative association between facility proximity and the fertility rate is stronger when (1) one's residence is on the walking routes from a facility toward its nearest rail station or bus stop or (2) the local private-car use is lower.

3 Data and Empirical Design

This section describes the data and empirical design used to examine the relationship between disability service facilities and local fertility. I first introduce the census mesh data and define the child–woman ratio, the local measure of fertility used in this paper. I then describe the disability service facilities and the construction of spatial exposure. I next present the baseline controls and the restrictions defining the common estimation sample. Finally, I set out the distance-band specification and the assumptions required for a causal interpretation. Appendix Table A.1

reports summary statistics for the main estimation sample. Full source citations, file identifiers, and construction details are provided in Appendix A.

3.1 Census mesh data and the fertility outcome

I use Japan's 2020 Population Census regional-mesh statistics. Regional meshes form a standardized latitude–longitude grid whose boundaries are independent of administrative divisions. Figure 1(a) shows the nationwide grid schematically and enlarges a parent 500m mesh to illustrate its four 250m cells arranged in a two-by-two grid.[15] Each 250m cell is a unit of observation in the main analysis, while the parent 500m mesh defines the local neighborhood, which I account for by the fixed effects in Section 3.3.

Using population counts by sex and five-year age group in each 250m cell, I define the main dependent variable for cell i, the children-to-woman ratio (CWR) as

$$\text{CWR}_i^{15\text{–}49} = 1000 \times \frac{\text{children ages 0–4}_i}{\text{women ages 15–49}_i}. \tag{1}$$

The numerator includes children aged between 0 and 4 of both sexes, while the women in the denominator is the number of women of childbearing age.[16] The CWR is a commonly-used measure of fertility rates at a spatially granular level, but note that the CWR does not necessarily equal an annual birth rate or a measure of completed fertility. In particular, the CWR is could be influenced by migration behavior that is not directly related to reproductive behavior. Section 4.3.2 examines the sensitivity of my results to migration.

I combine census counts across all 47 prefectures. To preserve the correspondence between population counts and individual mesh areas, I exclude both confidentiality-suppressed cells and cells receiving their aggregated counts. Eligible cells must contain at least 10 women ages 15–49; cells with no children ages 0–4 remain eligible and have a CWR of zero.

3.2 Facility locations and spatial exposure

Facility location data come from the 2021 National Land Numerical Information Welfare Facilities Data (P14), which publicizes the location of the welfare facilities in Japan. I retain 57,755 adult disability-related facility samples after dropping a few observations without enough locational accuracy. Note that I exclude facilities specifically for children with disabilities because their locations may respond directly to demand from families with children, and their services may affect those families through access to care.[17] Appendix A.2 documents more details on this data.

[15] I call the 500m mesh that contains the 250m mesh of interest as the "parent" mesh. I also use the words "mesh" and "cell" interchangably.

[16] Following the standard definition of the CWR, I define the childbearing age as 15–49. Using 20–39 definition does not change my conclusion (Section 5).

[17] Appendix A.2 reports the sensitivity analysis that adds these facilities, finding that my results are overall robust.

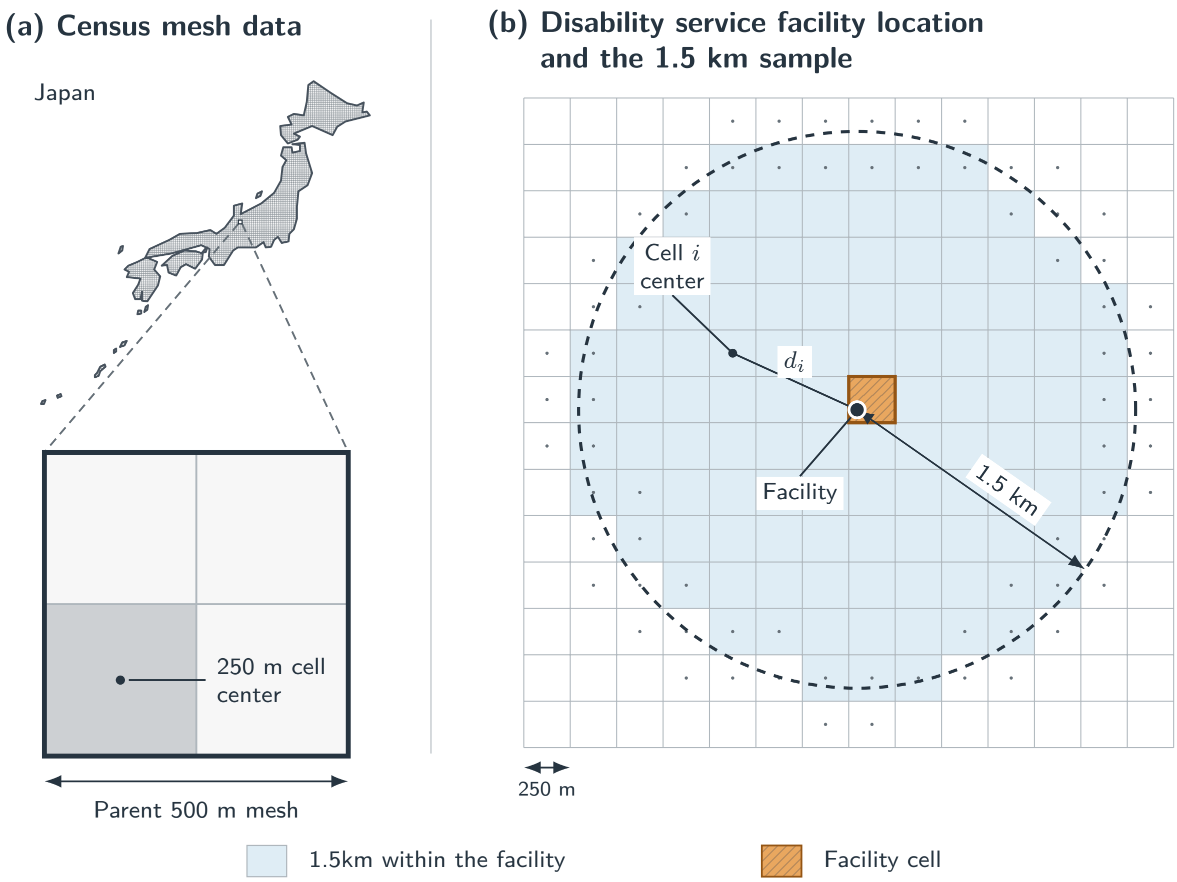

Figure 1: Census Meshes, Facility Locations, and the Spatial Sample

Notes: Panel (a) shows how each 500 m mesh divides into four 250 m cells. In panel (b), blue cells lie within 1.5 km of the facility, measured from their centroids; the orange hatched facility cell is excluded. The dashed circle marks the 1.5 km cutoff, and d_i is cell i's distance to the facility. The analysis assigns each cell to its nearest adult disability facility and applies the additional sample restrictions in the text. The maps are schematic and not to scale.

Japan's disability-welfare system supports people with physical, intellectual, and mental disabilities, including developmental disabilities. The welfare service facilites in my sample encompass residential support facilities and group homes, day-service and employment-support establishments, community-activity and welfare centers, and consultation or home-help offices. These services provide accommodation and daily-living assistance, daytime care and activities, employment support, or assistance with access to care (Ministry of Health, Labour and Welfare, 2018). The records therefore mix residential premises, activity sites, and service offices; users need not reside or attend activities at every recorded location. However, exactly identifying which facility focuses on which activity is difficult as many facility provides a menu of services.

Figure 1(b) illustrates the following sample selection procedure. I assign each 250m cell in the Census to its nearest admissible disability service facility using great-circle distance from the cell centroid. I keep cells less than 1.5 km away and groups distances into six 250 m bands, with 1.25–1.50 km as the reference.[18] To address the concern that the cell with the disability service facility may have mechanically lower fertility rates because the residents of the group home have lower fertility rates, I exclude every cell containing an admissible adult disability facility, to avoid mechanically linking the comparison to the population composition within facilities.[19]

After applying the population, confidentiality, and spatial restrictions, I require complete observations for the outcome and all ten baseline controls. I then recursively remove cells that are the sole remaining observation in either their nearest-facility group or their parent-500 m mesh. The resulting main estimation sample contains 190,747 cells assigned to 26,220 nearest facilities and 63,290 parent 500 m meshes. The assigned facilities are the subset of the 57,755 admissible points that serve as the nearest facility for at least one retained cell. All three main specifications use this same sample, so their coefficient differences reflect changes in conditioning rather than sample composition. The estimates therefore describe eligible neighborhoods within 1.5 km of these facilities.

3.3 Empirical specification and identification

Let $f(i)$ denote the nearest admissible facility assigned to cell i, $m(i)$ its unique parent-500 m mesh, and D_{ib} the five distance-band indicators: 0-250m, 250-500m, 500-750m, 750-1000m, 1000-1250m. The distance of 1250-1500m is used as the reference category.

The preferred specification for the distance analysis in Section 4.1 is:

$$\mathrm{CWR}_i = \sum_{b=0}^{4} \beta_b^{(3)} D_{ib} + X_i'\gamma + \alpha_{f(i)} + \delta_{m(i)} + u_i. \tag{2}$$

Here, nearest-facility fixed effects $\alpha_{f(i)}$ absorb differences across facility catchments, while

[18] Using cells within 2km from the nearest facility does not change my results (see Section 5).

[19] Consistent with this, not exclusing these cells slightly strengthens my results (see Section 5).

parent-500 m fixed effects $\delta_{m(i)}$ absorb characteristics shared by adjacent census cells. X_i is the ten-variable baseline control vector that I desecribe in the next paragraph. In my regression, I try a specification that omits the parent-500 m fixed effects and baseline controls, a specification that omits only the baseline controls, and a full specification with both fixed effects and the baseline controls.

The ten baseline controls are meant to capture heterogeneous location characteristicsm combinining 2020 Census demographic, education, and housing data. Four demographic and education measures are the natural logarithm of population density, the share of total population age 65 or older, the approximate mean age of women ages 15–49, and the university-graduate share. Population density uses each cell's geographic area and is measured in residents per square kilometer before taking logs. The university-graduate share divides university and graduate-school graduates by all school graduates ages 15 or older, regardless of school level, pooling men and women. Three zoning indicators identify residential, commercial, and industrial classifications at the cell centroid. Their omitted category includes both other designated zones and cells outside the zoning data's coverage. Three housing-form shares measure row houses, apartment buildings, and other or unstated building forms among general households living in housing, with detached houses omitted. I require that for a cell to be included in my analysis sample, all of these ten control variables are observed. Appendix A.4 gives detailed variable definitions.

The baseline specifications are estimated by weighted least squares using the number of women ages 15–49 as analytic weights, aiming to replicate all women at the childbearing age in Japan as the population. Standard errors in Equation (2) are clustered two ways by nearest facility and parent-500 m mesh (Cameron et al., 2011). In a simpler specification that uses the facility fixed effects only, standard errors are clustered by nearest facility. The coefficient $\beta_0^{(3)}$ in Equation (2) compares the 0–250 m and 1.25–1.50 km bands.

4 Main Results

4.1 Proximity to disability service facility and the fertility rate

Table 1 and Figure 2 report the estimation results of specification (2): Column (1) is the case of the facility fixed effects only, Column (2) is the case of the facility and parent 500m mesh fixed effects, and Column (3) further adds the baseline controls. Overall, all of these three specifications reveal a lower CWR close to disability service facilities. In the full specification in Column (3), cells within 250 m have 7.39 fewer children ages 0–4 per 1,000 women ages 15–49 than cells 1.25–1.50 km away (standard error 3.22, $p = 0.022$). The difference is equivalent to 3.9 percent of the weighted sample mean CWR of 191.86, which is consistent with a meaningfully large effect on the fertility rate. In Column 3, the estimated 250–500 m and 500–750 m dummies are −6.36 and −6.39, respectively, both significant at the 5 percent level, while dummies further away are indistinguishable from zero.[20] This pattern may suggest that the impact of the welfare service facility may attenuate over distance but reach up to 0.75km. This pattern is consistent with the localized association in Hypothesis 1: the disability service facility promotes incidental social contacts with people with disability and their caregivers and this may lower the fertility rate.

With this baseline result that the fertility rates are lower around the disablity service facilities, I extend my analyses in two ways. First, Section 4.2 examines additional proxies of the incidental social contact to highlight that the lower fertility likely stems from more incidental social contacts. Second, Section 4.3 assesses alternative explanations through placebo analyses, explicitly accounting for migration, land price, and safety levels, and sensitivity to unobserved confounding.

Table 1: CWR and the Distance from the Nearest Disability Facility: Baseline Results

Distance band (km)	(1)	(2)	(3)
0–0.25	-6.516^{***}	-8.014^{**}	-7.394^{**}
	(1.980)	(3.438)	(3.216)
0.25–0.50	-2.475	-5.630^{*}	-6.358^{**}
	(1.903)	(3.297)	(3.085)
0.50–0.75	-0.812	-5.587^{*}	-6.389^{**}
	(1.891)	(3.187)	(2.968)
0.75–1.00	1.011	-2.877	-3.880
	(1.906)	(2.895)	(2.694)
1.00–1.25	-0.830	-2.680	-2.577
	(1.914)	(2.223)	(2.118)
1.25–1.50 (reference)	0	0	0
Facility fixed effects	Yes	Yes	Yes
Parent-500 m fixed effects	No	Yes	Yes
Baseline controls	No	No	Yes
Observations	190,747	190,747	190,747

Notes: Entries are differences in the 2020 CWR (children ages 0–4 per 1,000 women ages 15–49) relative to 1.25–1.50 km. All columns use the same sample, exclude cells containing adult disability facilities, and weight by the number of women ages 15–49. Baseline controls are defined in Section 3.3. Standard errors in parentheses are clustered by nearest facility in column (1), and by facility and parent-500 m mesh in columns (2)–(3). $^{*}p < 0.10$, $^{**}p < 0.05$, $^{***}p < 0.01$.

[20] This pattern is similar in Column 2, but Column 1 does not exhibit statistical significance for these dummies.

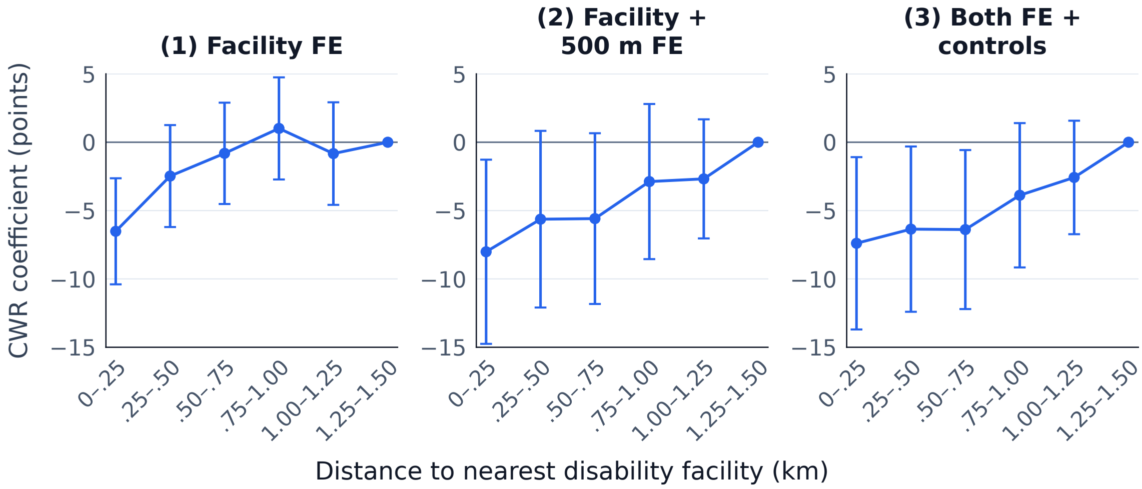

Figure 2: CWR and the Distance from the Nearest Disability Facility: Graphical Illustration

Notes: Points show the distance-band coefficients in Table 1, relative to 1.25–1.50 km; bars show 95 percent confidence intervals. CWR is children ages 0–4 per 1,000 women ages 15–49. All three specifications use the same 190,747 cells, weighted by women ages 15–49. Standard errors are clustered by nearest facility in column (1) and by facility and parent-500 m mesh in columns (2) and (3).

4.2 Opportunities for incidental social contact

Hypothesis 2 links the distance gradient to opportunities to see people with disabilities and accompanying caregivers on neighborhood streets. I examine two complementary features of this environment: modeled walking routes to transit and neighborhood reliance on private cars.

4.2.1 Transit-route direction

To evaluate the route prediction in Hypothesis 2, I combine the location data of railway stations and bus stops. As in Figure 3(a), I define the route between these public transportation points and the disability service facilities, motivated by the idea that they are likely to walk between these two points on the street and become visually salient to residents along the way. Using the OpenStreetMap walking network, for each facility, I compute paths to its nearest station and bus stop.[21] The actual-path indicator equals one when a cell's rectangle intersects an available path assigned to its nearest facility., as indicated in Figure 3(a). The main specification takes the union of the available station-derived and bus-derived paths; if neither is available, the indicator is missing.

In order to mitigate the cocnern that the path to the disability service facility has certain confounding characteristics, I compare the results with the "placebo paths" that lead to the same disability service facility but from hypothetical train or bus stations. Figure 3(b) illustrates the construction of the placebo paths. I first rotate each train or bus station around the facility by 90, 180, or 270 degrees, recompute the walking path, and apply the same union rule. Rotation

[21] In Appendix Table B.2 I report the results using the straight-line paths between the facility and the nearest train or bus stations, which does not reply on the walking network. The results are similar.

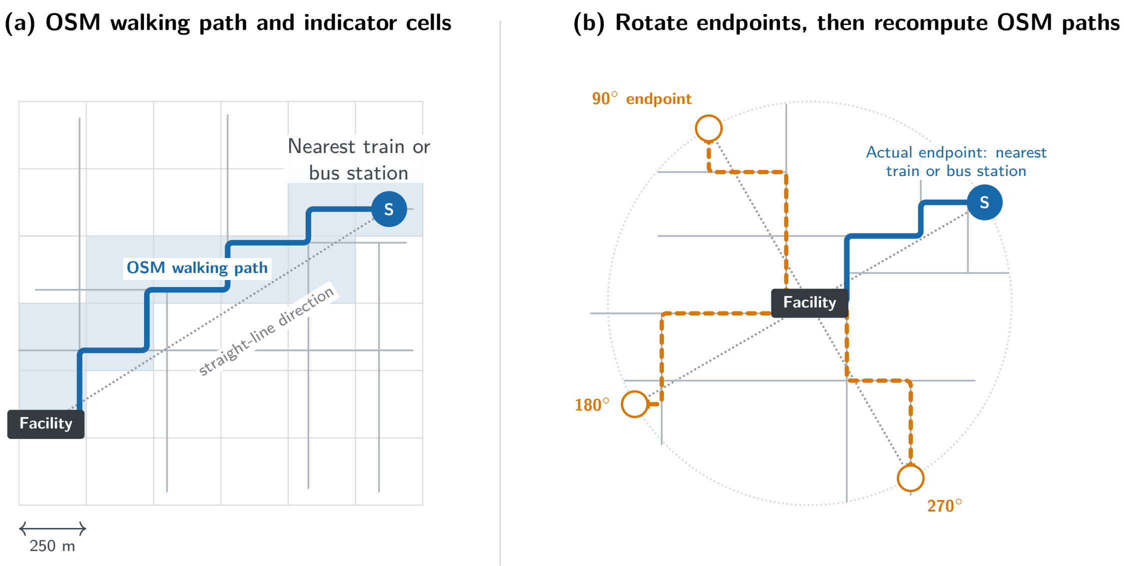

Figure 3: Construction of OSM-Routed Actual and Rotated Transit Paths

Notes: Panel (a) shows a walking path from a facility to its nearest station or bus stop. A shaded cell intersects an available path from its assigned facility. Facility-containing cells are shown for illustration and excluded from estimation. In panel (b), the destination is rotated by 90, 180, or 270 degrees around the facility, and the walking path is recalculated. Rotation keeps the straight-line distance unchanged, but the walking distance can change. Appendix A.5 describes path construction and availability. The diagram is not to scale.

preserves the straight-line endpoint distance, while routed lengths can change depending on the road network. See Appendix A.5 for more details of the procedure.

In my analysis, I add the actual-path and three rotated-path indicators to my baseline model (2):

$$\begin{aligned} \mathrm{CWR}_i = \sum_{b=0}^{4} \beta_b D_{ib} + \sum_{q \in \{A,90,180,270\}} \theta_q R_i^q \\ + X_i' \gamma + \alpha_{f(i)} + \delta_{m(i)} + u_i . \end{aligned} \tag{3}$$

Here R_i^A denotes the actual station-or-bus path indicator, while R_i^{90}, R_i^{180}, and R_i^{270} denote the rotated-path indicators defined above. Thus, θ_A measures the actual-path CWR difference conditional on radial distance and the other paths, while $\theta_A - (\theta_{90} + \theta_{180} + \theta_{270})/3$ compares the actual direction with the average rotated direction. Weighting and clustering are conducted similarly as Section 3.3. Appendix B.1 provides further details.

Figure 4 reports the coefficients of the actual and placebo routes from the specification with the facility and parent 500m mesh fixed effects and baseline controls (see Appendix Table B.1 for full regressioon results). The actual-path coefficient is -2.80 (standard error 0.93, $p = 0.003$) and is 3.42 CWR points lower than the average coefficient on the three rotated paths (standard error 1.10, $p = 0.002$).[22] As clarified in Table B.1, the actual-path coefficient is negative in all three specifications. This supports the part o1 of Hypothesis 2 in Section 2.

[22]Table B.1 shows that the distance dummies from the disability service facilities continues to exhibit the similar pattern as Table 1.

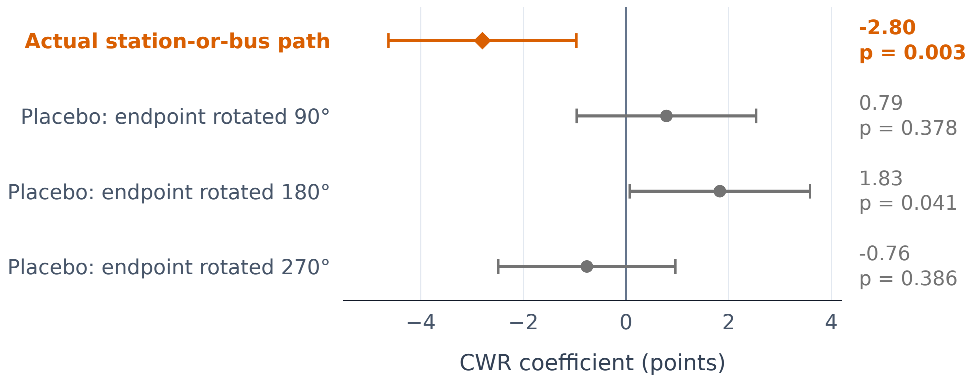

Figure 4: Estimated CWR Differences Along Actual and Placebo OSM Routes

Notes: Points show CWR differences for cells intersecting each path, estimated jointly in column (3) of Appendix Table B.1; bars are 95 percent confidence intervals. The model includes the five distance bands, facility and parent-500 m fixed effects, and ten baseline controls. It uses 190,445 cells weighted by women ages 15–49, with standard errors clustered by facility and parent-500 m mesh.

Appendix Tables B.3 and B.4 separate the station-derived and bus-derived paths, respectively. The station-only actual-path coefficients are −4.34, −2.92, and −2.63, all significant at the 1 percent level. The bus-only coefficients are −3.72 ($p < 0.001$), −2.47 ($p = 0.062$), and −1.13 ($p = 0.356$). Thus, the negative actual-path association is more precisely estimated for stations. The bus-only association becomes small and imprecise after including baseline controls, but the estimates' magnitudes are overall similar to those of the buses. This is consistent with the interpretation that both routes to train stations or bus stations create similar opportunities for the incidental social contact, leading to lower fertility rates.

4.2.2 Local private-car use

Private-car use provides another check of the importance of the incidental social contact: if car travel reduces incidental contact on streets and around transit stops, the negative impact on the fertility should be weaker where car use is higher, and vice versa.

The 2020 Population Census record the mode of transportation in commuting at the parent-500 m level. I use the car use rate in commuting as a proxy of the local car dependence (see Appendix A.4 for the variable construction).

I allow the distance profile in the model (2) to vary with the car use rate as follows:

$$\begin{aligned}\mathrm{CWR}_i = \sum_{b=0}^{4} \beta_b D_{ib} + \sum_{b=0}^{4} \theta_b z_{m(i)} D_{ib} \\ + X_i'\gamma + \alpha_{f(i)} + \delta_{m(i)} + u_i.\end{aligned} \tag{4}$$

Here $z_{m(i)} = (c_{m(i)} - \bar{c}_w)/0.10$, where $c_{m(i)}$ is the share of commuters using private cars and $\bar{c}_w \simeq 0.42982$ is its sample mean with the number of women at the childbearing age as weights. An increase of one in $z_{m(i)}$ therefore represents 10 percentage points more car use. Because

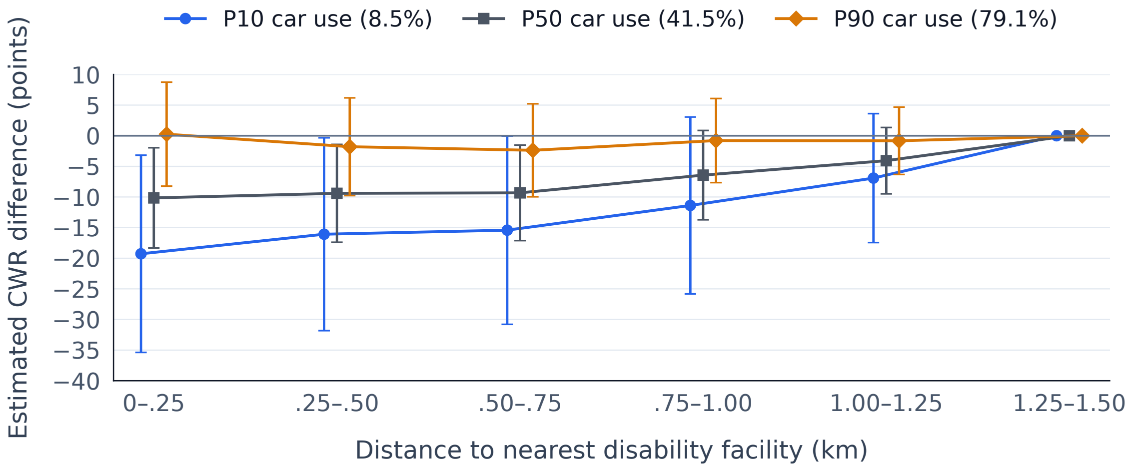

Figure 5: The disability facility and the CWR by private-car-use rate

Notes: All three profiles come from one regression with a separate car-use interaction for each of the five distance bands (Equation 4). Points compare CWR with the 1.25–1.50 km band at the women-weighted 10th, 50th, and 90th percentiles of car use (8.5, 41.5, and 79.1 percent). Bars are pointwise 95 percent confidence intervals, accounting for uncertainty in both main and interaction coefficients. The sample (190,747 cells), controls, fixed effects, weights, and clustering follow column (3) of Table 1.

the the car-use rate is measured at the parent 500m mesh level, its direct effect is absorbed by the parent-500 m fixed effects. θ_b measures the change in the band-b CWR difference per 10-percentage-point increase in car use. Weighting and clustering follow Section 3.3.

Figure 5 evaluates this specification at the 10th, 50th, and 90th percentiles of car use (8.5, 41.5, and 79.1 percent). The estimated nearest-band differences relative to 1.25–1.50 km are -19.28, -10.15, and 0.26, respectively; the 10th-minus-90th-percentile contrast is -19.53 points. The estimate at the 10th percentile is more than twice as large as the baseline estimate in Table 1, amounting to about 10% decline of the CWR. In contrast, the estimate at the 90th percentile is near zero, consistent with the interpretation that car travels limit the opportunities for incidental social contacts.

Taken together, I find evidence supporting Hypothesis 2 in Section 2. More opportunities for incidental social contacts with people with disability and their caregivers, proxied by the routes between the facility and public transportation points or the local car dependence rate, tend to predict lower fertility rates.

4.3 Assessing alternative explanations

I assess alternative explanations for the proximity association in two steps. Section 4.3.1 examines pre-entry CWR patterns and proximity to elderly care facilities. Section 4.3.2 evaluates residential sorting, land prices, and recorded crime, and concludes with a sensitivity analysis for unobserved confounding.

4.3.1 Placebo analyses

I use two placebo analyses to assess pre-existing local fertility patterns and proximity to welfare facilities more generally. The first examines whether the 2015 fertility rate varies with proximity to candidate future disability facilities observed in 2021, after screening their locations against both the 2011 and 2015 welfare-facility records. The second examines whether a similar CWR profile appears around facilities primarily providing care associated with aging.

Future entry of disability facilities placebo. A potential concern is that areas that host the disablity service facilities have certain unobserved location characteristics and they are correlated with the lower fertility rate. For example, neighborhood opposition can constrain the establishment of disability service facilities in Japan (Okahara et al., 2022). If opposition is stronger in neighborhoods with more young children, facilities may locate in areas with lower pre-existing CWRs.

To address such a concern, this placebo test asks whether the 2015 CWR already displayed a distance gradient around these candidate future facilities. This placebo analyzes the relationship between the 2015 CWR and adult-disability facility records observed in the 2021 P14 data that pass historical screens using both the 2011 and 2015 data. The screens exclude candidates within 250 m of a historical welfare-facility point or with a qualifying name or address match.[23] These locations may share characteristics that attract disability service facilities. If the candidates represent facilities that opened after 2015, an incidental-contact mechanism should not produce a 2015 CWR gradient around them. The historical screen is conservative: nearby records of other welfare facilities also trigger exclusion, and absence from the two historical datasets does not establish an opening date. I use the same specification as the main specification in Table 1, and Appendix B.3.1 provides the specification details.

Figure 6, Panel A reports the results (see Appendix Table B.5 for the full regression results). The estimated 0–250 m coefficients are −0.59, 0.89, and 0.11 across the three specifications, which are substantially smaller in absolute value than the main estimates in Table 1 and statistically indistinguishable from zero.[24] The 250–500 m and 500–750 m coefficients are also close to zero across the three specifications. This placebo provides no evidence of a comparable negative pre-existing CWR gradient around the screened candidate locations; its interpretation remains conditional on the historical datasets' coverage and the absence of verified opening dates.

Elderly care facility placebo. If facilities primarily providing care associated with aging had a similar negative effect on fertility, then incidental social contact with people with disability would be less likely to be the primary reason. For example, it is possible that areas around

[23] Appendix A.6 defines the matching rules, harmonizes coordinate systems, and documents separate checks for historical points with unavailable coordinate corrections.

[24] In contrast, the separate 2015 cross-sectional replication in Appendix Table B.6 produces estimates similar to the main estimates based on the 2020 data in Table 1.

welfare facilites tend to be preferred by those with weaker fertility intentions. I now check this possibility by examining the impact of the elderly care facilities on fertility rates.

The elderly care facility placebo uses 130,545 admissible facilities from the same 2021 P14 dataset. The categories encompass nursing and residential homes, long-term-care health and medical facilities, day-service and short-stay centers, and community or home-care support services. These facilities share the neighborhood presence of welfare and caregiving services while primarily addressing needs associated with aging. I reconstruct distances and facility-cell exclusions around this universe in the similar way to the main analysis and use the same empirical specification (2) to estimate the impact of the proximity to the elderly care facilities on the CWR. Appendix A.2 gives more details.

Panel B of Figure 6 reports the results (see Appendix Table B.7 for the full regression results). In the fully controlled specification, the coefficients from 0–250 m through 1,000–1,250 m are 2.09, 0.16, 1.30, −0.77, and −2.93. The nearest 0-250m dummy has a standard error of 3.79 and $p = 0.582$, and none of the five controlled coefficients is statistically significant. Overall, the relationship in Table 1 is driven by the specific aspect of the disability service facilities, which is not seen in the elderly care facilities, another primary type of welfare facilities.

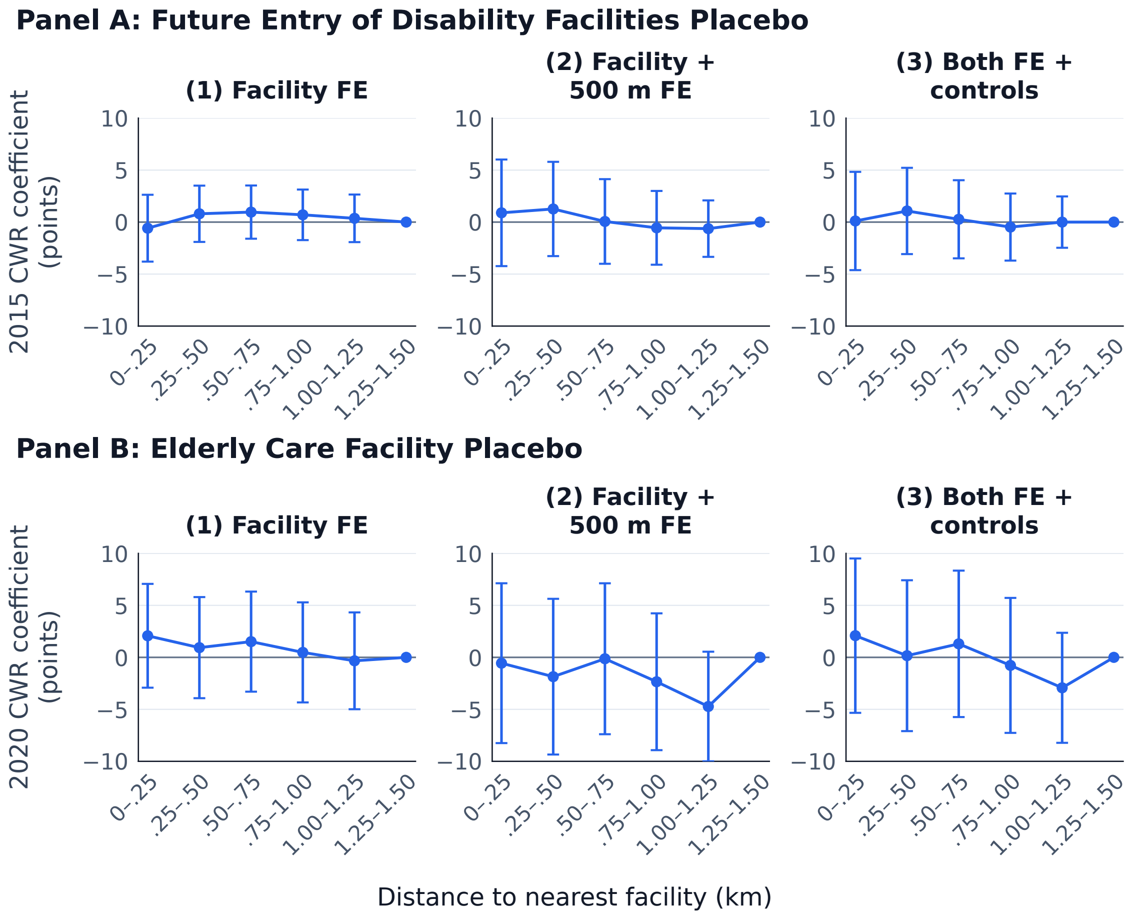

Figure 6: Placebo Tests

Notes: Points show CWR differences from the 1.25–1.50 km band; bars are 95 percent confidence intervals. Panel A uses the 2015 CWR around candidate future disability facilities selected from the 2021 records using the 2011 and 2015 historical checks (Appendix A.6; N = 138,229). Cells containing candidates are excluded; other facility cells remain eligible. Panel B uses the 2020 CWR around elderly care facilities and excludes cells containing them (N = 192,156). Each panel uses a common sample, weighted by women ages 15–49. Specifications and clustering follow Appendix Tables B.5 and B.7; column (3) uses nine controls in Panel A and ten in Panel B.

4.3.2 Accounting for confounders

Although I have incorporated flexible fixed effects (i.e., nearest facility and parent 500m mesh fixed effect) and several control variables regarding socioeconomic conditions, housing, and zoning, a concern that some unobserved counfounders may drive my results could remain. In this section, I consider the role of three potential confounders: migration, land prices, and safety levels. As discussed below, I find that these factors play, at most, a limited role in explaining the negative association between the disability service facilities and the fertility rate.

Table 2: Sensitivity to Controlling for Residential Sorting, Land Prices, and Theft

Distance band (km) / regressor	(1)	(2)	(3)
Panel A: Net child migration rate			
0–0.25	−4.766**	−7.020**	−7.002**
	(1.980)	(3.470)	(3.251)
0.25–0.50	−1.634	−5.339	−6.491**
	(1.892)	(3.337)	(3.134)
0.50–0.75	−0.280	−5.456*	−6.568**
	(1.878)	(3.231)	(3.018)
0.75–1.00	1.152	−3.456	−4.675*
	(1.890)	(2.931)	(2.743)
1.00–1.25	−1.141	−2.994	−3.148
	(1.892)	(2.271)	(2.174)
1.25–1.50 (reference)	0	0	0
Net child migration rate (5–9 as of 2020)	0.077**	0.068**	0.062***
	(0.030)	(0.027)	(0.024)
Net child migration rate (10–14 as of 2020)	0.020	0.004	−0.011
	(0.013)	(0.012)	(0.011)
Observations	173,438	173,438	173,438
Panel B: Residential land price			
0–0.25	−6.390***	−7.984**	−6.744**
	(2.000)	(3.439)	(3.218)
0.25–0.50	−2.368	−5.605*	−5.786*
	(1.920)	(3.297)	(3.086)
0.50–0.75	−0.739	−5.567*	−5.951**
	(1.899)	(3.187)	(2.969)
0.75–1.00	1.046	−2.866	−3.644
	(1.907)	(2.897)	(2.699)
1.00–1.25	−0.816	−2.675	−2.455
	(1.915)	(2.223)	(2.121)
1.25–1.50 (reference)	0	0	0
Predicted log residential land price	−2.005	−0.674	−17.156***
	(2.911)	(4.751)	(4.436)
Observations	190,747	190,747	190,747
Panel C: Recorded theft			
0–0.25	−6.806***	−8.515**	−7.750**
	(2.002)	(3.470)	(3.245)
0.25–0.50	−2.777	−6.103*	−6.722**
	(1.926)	(3.330)	(3.115)
0.50–0.75	−1.046	−5.931*	−6.665**
	(1.913)	(3.219)	(2.997)
0.75–1.00	0.846	−3.120	−4.048
	(1.927)	(2.925)	(2.719)
1.00–1.25	−0.796	−2.563	−2.389
	(1.933)	(2.241)	(2.134)
1.25–1.50 (reference)	0	0	0
Theft rate (per 1,000 residents)	−0.126***	−0.042	−0.023
	(0.047)	(0.047)	(0.044)
Observations	185,995	185,995	185,995
Nearest-facility fixed effects	Yes	Yes	Yes
Parent-500 m fixed effects	No	Yes	Yes
Baseline controls (ten variables)	No	No	Yes

Notes: The outcome is the 2020 CWR, measured as children ages 0–4 per 1,000 women ages 15–49. Distance coefficients compare each band with 1.25–1.50 km. Each panel adds the named controls to the three specifications in Table 1 and holds the sample fixed across columns. Panel A requires positive 2015 child cohorts and all four sorting measures; Panel B uses the main sample; Panel C requires at least 50 residents per cell. Migration rates are in percentage points, land price is predicted log price, and theft is records per 1,000 residents (Appendix A). Regressions exclude adult-facility cells and weight by women ages 15–49. Standard errors in parentheses cluster by nearest facility in column (1), and by facility and parent-500 m mesh in columns (2)–(3). $^{*}p < 0.10$, $^{**}p < 0.05$, $^{***}p < 0.01$.

Selective migration. An important concern for using the CWR as a fertility measure is that selective migration (i.e., residential sorting) can contaminate it by altering the relative numbers of young children and reproductive-age women without reproductive behavior. Specifically, the CWR falls if households with more young children per woman are more likely to leave or less likely to enter a neighborhood. Therefore, a change in residential composition could lower the CWR around the disability facility if it selectively attracts those with fewer children.[25]

To address this concern, I construct a proxy of the selective migration as follows. Note first that the number of children aged 0–4 changes by two factors: the fertility rates and the migration of children.[26] My aim is to isolate the change due to the migration channel, but I cannot directly observe it in the Population Census because it is conducted every five years and the available migration variable is at the municipality level, which is a far more aggregate spatial unit than the 250m cell I use in this paper. Therefore, to proxy for children's net migration tendency, I follow changes in the number of two cohorts between the 2015 and 2020 Censuses: the cohorts with ages 5–9 and 10–14 in 2020. Since these changes do not reflect fertility decisions because these cohorts were already born, they reflect only the migration tendency. I therefore call them as "net migration rates of children." These measures proxy migration relevant to the 2020 CWR insofar as older and younger children's migration shares common determinants, implying that controlling for them would allow me to extract the impact of the disability service facilities on the fertility decisions.

Panel A of Table 2 includes both child migration rates. The nearest-band coefficients are −4.77, −7.02, and −7.00 across the three specifications (standard errors 1.98, 3.47, and 3.25), all negative and significant at the 5 percent level. The relevant baseline is the regression without these rates on the same 173,438 cells: its preferred coefficient is −8.05. Thus, conditioning on measured net child migration attenuates the preferred estimate modestly while leaving most of the negative association in place.

To further assess the role of migration, I also control for the log change in the number of women ages 15–49 and the female recent-mover share, defined in Appendix Equations (A.3) and (A.4). Changes in the female population may matter because facility proximity could influence where women of childbearing age live, thereby affecting the denominator of the CWR. I include the female recent-mover share because residential moves and childbearing decisions are interrelated, and moves may occur in anticipation of future births (Kulu and Steele, 2013; Ermisch and Steele, 2016; Anstreicher and Venator, 2026). In Panel A of Appendix Table B.8, including them alongside both child migration rates leaves a preferred nearest-band coefficient of −6.25 (standard error 2.84, $p = 0.028$). The coefficients remain negative in all three speci-

[25]Note that proportional changes in children and women leave it unchanged, implying that the volume of migration itself does not necessarily translate into the bias in the CWR.

[26]Precisely speaking, it is also affected by the infant mortality rate. I ignore this in this paper because child mortality in Japan is very low: the 2020 life tables imply survival above 99.7 percent from birth to age 5 and above 99.9 percent from age 5 to age 15 for both sexes (Ministry of Health, Labour and Welfare, 2021). Therefore, its spatial variation quantiatively cannot explain the variation in the CWR found in Section 4.

fications,. Taken together, controlling for various migration-related factors does not explain a large part of the decline in the fertility rate around the disability service facilities.

Residential land prices. Housing markets can affect fertility through both the cost of accommodating children and households' financial resources (Lovenheim and Mumford, 2013; Dettling and Kearney, 2014). At the same time, proximity to disability service facilities could be associated with local prices through changes in housing demand. Indeed, although the evidence is mixed, the literature of estimating the impact of group homes on housing prices suggests that such an impact could exist (Gabriel and Wolch, 1984; Farber, 1986; Colwell et al., 2000; Galster et al., 2004). If so, the disability service facilities could affect the fertility rate through housing market, not through the incidental social contacts. I examine this possibility by examining the robustness of my results to controlling for the housing market responses.

I examine this possibility by constructing a spatially granular land price estimates for the 250m cells Specifically, for each centroid of the cell, I pick the two nearest residential-use assessment points in the 2020 Land Price Publication and Prefectural Land Price Survey. I then construct the predicted land price by weighting log prices by inverse squared distance; Appendix A.8 gives the details.

All three columns retain the 190,747-cell main sample. In the fully controlled specification in column (3), the 0–250 m coefficient moves from −7.39 to −6.74 (standard error 3.22, p = 0.036), a reduction of 8.8 percent in absolute magnitude. The remaining distance-band estimates also stay close to the baseline profile. The negative CWR association therefore changes only modestly after conditioning on measured local prices; Tables 1 and 2 report the profiles before and after adjustment.

Panel B of Table 2 reports the regression results while additionally controlling for the predicted land prices.[27] Adding land price changes the nearest-band coefficient from −6.52 to −6.39 in column (1) and from −8.01 to −7.98 in column (2). In the fully controlled specification in column (3), the 0–250 m coefficient moves from −7.39 to −6.74 (standard error 3.22, p = 0.036), a reduction of 8.8 percent in absolute magnitude. Overall, land prices do not explain most of the negative fertility rates near the disability service facilities.

Safety level. An alternative explanation for the lower fertility rate around the disability service facilities is that concerns about children's safety discourage childbearing. Prospective parents who expect a child to face violence or other dangers in the neighborhood may postpone or forgo a birth, or they may actually increase fertility intentions (Guerra-Cújar et al., 2024), although the effect could be the opposite once general-equilibrium effects are taken into account (Awaworyi Churchill et al., 2022). Child-safety concerns also appear in opposition to disability facilities

[27] Given the mixed evidence in the literature about the impact of disability facilities on land prices, Appendix Table B.9 treats predicted log land price as the outcome. The nearest-band coefficients are positive across the three specifications, at 0.0627, 0.0433, and 0.0379; the preferred estimate corresponds to 3.86 percent higher predicted residential land prices. The higher price is consistent with Farber (1986) and Galster et al. (2004).

in Japan. In a documented campaign in Yokohama, opponents of a disability group home displayed banners urging residents to “protect children’s safety” (Okahara et al., 2022, p. 44). Such rhetoric makes perceived neighborhood danger a relevant alternative explanation, but does not establish that facilities or their users increase crime.

While this is a possibility, official crime statistics in Japan does not show a strong association betwen crime rates and the disability service facilities. I use two complementary datasets to check this. First, I use the nation-level theft occurance data. While this covers the entire Japan and the spatial unit is granular, the data availability is limited only to the thefts. Second, I use the crime data of Tokyo, which have the similar spatial granularity but cover not only thefts but other crimes, such as murders and bulgrary. In both datasets, the association between crimes and the disability service facility is null, except that Tokyo’s data suggest that violent or serious offences and burglary are *less* likely to occur near the disability service facilities. See Appendix B.6.1 and B.6.2 for more details.

Consistent with the weak association between crimes and the disability service facility, controlling for crimes does not explain the lower fertility rate around it. Panel C of Table 2 adds the 2020 recorded theft rate per 1,000 residents to each of the three CWR specifications.[28] In the fully controlled specification in column (3), adding the theft rate shifts the 0–250 m coefficient by less than 0.002 CWR point, from -7.751 to -7.750 (standard error 3.245, $p = 0.017$). The next two distance-band coefficients also remain negative and statistically significant at the 5 percent level. Thus, controlling for observed theft rates leaves the negative CWR profile essentially unchanged. Overall, although I cannot fully rule out the possibility that crimes and other incidents not appearing the official crime records around the disability service facility affect the fertility rates, they find essentially no support in the official crime statistics.

Sensitivity to unobserved confounding. In order to further mitigate the concern that the unobserved confounders drive my results, Appendix Table B.13 applies the proportional-selection analysis of Oster (2019), using sorting, land price, and recorded theft as separate observed benchmarks. Assuming equal proportional selection and an unobserved conditional R^2 gain equal to the observed gain yields adjusted coefficients of -5.952 and -4.457 for sorting, -6.095 for land price, and -7.748 for theft. All remain negative under this calibration. Overall, my conclusion is robust to considering additional unobserved confounders.

5 Robustness checks

This section provides robustness results on the sample definition, the fertility measure, or the method of estimation and inference. The appendix reports the full results.

Facility-containing cells. My main analysis excluded from the sample the cell in which a

[28] I chose the theft variable because it is available nationwide.

disability service facility is located to avoid the concern that residents of group homes have mechanically lower fertility rates. Table B.14 restores cells containing adult disability service facilities. The preferred 0–250 m coefficient is −7.82, compared with −7.39 in the main sample, and the distance profile remains similar. Excluding facility-containing cells therefore does not drive the result.

Alternative CWR denominator. My main definition of the CWR used the ages between 15 and 49 as the childbearing age. Table B.15 instead uses women ages 20–39 in the denominator, which more focuses on the prime age of childbearing. On the same 140,679 cells, the preferred nearest-band coefficient is −18.78 (standard error 5.88), compared with −10.78 using women ages 15–49. The magnitudes are not directly comparable because both the denominator changes, but the association remains negative in all three specifications.

Two-kilometer estimation window. As seen in Figure 1, I restricted the smaple to cells within 1.5km from the disability service facility. Table B.16 extends the sample to 2 km while retaining 1.25–1.50 km as the reference band. The preferred nearest-band coefficient is −7.48, close to the main estimate. Neither of the two added outer-band coefficients is statistically significant, implying that the 1.5km threshold is large enough to capture the relevant spatial spillovers.

Spatial inference. While I have accomodated spatial correlation of standard errors by clustering at the nearest facility and the parent 500m mesh level, it does not accomodate spatial autocorrelation across different clusters. Table B.17 allows such spatial autocorrelation using Conley standard errors (Conley, 1999). Using this method does not change the point estiamtes. In terms of standard errors, with distance cutoffs of 0.5, 1, and 2 km, the nearest-band coefficient remains significant at the 5 percent level; the corresponding standard errors are 2.95, 3.14, and 3.28.

PPML specification. To assess robustness to the functional form, Table B.18 estimates the number of children using Poisson pseudo-maximum likelihood, with the number of women as the exposure (Santos Silva and Tenreyro, 2006). This allows proportional rather than additive differences and accommodates zero child counts. The preferred estimate implies a 3.08 percent lower child–woman rate within 250 m ($p = 0.054$), which is comparable to the magnitude of the main estimate disucussed in Section 4. Appendix B.8 describes more details.

6 Conclusion

This paper proposes a new determinant of fertility decisions: the perceived probability and cost of having a child with a disability. Building on the idea that incidental social contact with people with disabilities and their caregivers could make them salient, I investigate the relationship between the fertility rate and the disability service facilities, which would induce more opportunities of such incidental social contacts. Using spatially-granular census data in Japan, I find a lower child–woman ratio near disability service facilities. In the preferred specification, cells within 250 m have 7.39 fewer young children per 1,000 women of childbearing age than cells 1.25–1.50 km away, or 3.9 percent of the weighted sample mean. Similar negative differences extend through 750 m. Two spatial patterns further support the role of incidental social contact. First, conditional on facility distance, the fertility rate is lower along walking routes to transit destinations. The fertility rate around the disability service facilities is also lower where private-car use is lower. Both cases lead to more chances for people to observe people with disability and their caregivers on the street, and hence more incidental social contacts. Placebo tests based on the new entry of the facilities and elderly care facilities do not reproduce the main negative profile. Moreover, adjustments for selective migration, land prices, or safely levels leave most of the association in place, reinforcing the possibility that incidental social contacts with people with disability and their caregivers cause the fertility decline around the disability service facilities.

The findings suggest that perceived disability risk and anticipated caregiving demands may influence childbearing. While my results point to the role of incidental social contacts, the importance of other determinants of the anticipated disability risk or caregiving needs, such as education or media, remains for future research. At the same time, my result also suggests that the welfare system to support families with disabled children may have an *ex ante* insurance value as well as benefits for families already providing care. Confidence that financial assistance and care services will be available could ease uncertainty about parenthood, including for people who never use those services, and it might result in a higher fertility rate.

References

Allport, Gordon W., *The Nature of Prejudice*, Reading, MA: Addison-Wesley, 1954.

Anstreicher, Garrett and Joanna Venator, "To Grandmother's House We Go: Informal Childcare and Female Labor Mobility," *International Economic Review*, 2026, *67* (3), 1043–1068, doi: 10.1111/iere.70067.

Ashraf, Nava, Maxim Bakhtin, Erica Field, Alessandra Voena, and Roberta Ziparo, "Gendered Spheres of Learning and Household Decision-Making over Fertility," *The Review of Economic Studies*, 2026, rdag020, doi: 10.1093/restud/rdag020.

Asuman, Derek, Tinna Laufey Ásgeirsdóttir, and Johan Jarl, "Anxious Dads and Depressed Moms: Child Disability and the Mental Health of Parents," *Health Economics*, 2025, *34* (7), 1326–1349, doi: 10.1002/hec.4962.

Atkin, David, M. Keith Chen, and Anton Popov, "The Returns to Face-to-Face Interactions: Knowledge Spillovers in Silicon Valley," NBER Working Paper 30147, National Bureau of Economic Research, June 2022, doi: 10.3386/w30147, url: https://www.nber.org/papers/w30147.

Awaworyi Churchill, Sefa, Russell Smyth, Trong-Anh Trinh, and Siew Ling Yew, "Local Crime and Fertility," *Journal of Economic Behavior & Organization*, 2022, *200*, 312–331, doi: 10.1016/j.jebo.2022.06.019.

Balbo, Nicoletta and Nicola Barban, "Does Fertility Behavior Spread among Friends?," *American Sociological Review*, 2014, *79* (3), 412–431, doi: 10.1177/0003122414531596.

Becker, Gary S., "An Economic Analysis of Fertility," in *Demographic and Economic Change in Developed Countries*, New York: Columbia University Press, 1960, pp. 209–240.

Becker, Gary S. and H. Gregg Lewis, "On the Interaction between the Quantity and Quality of Children," *Journal of Political Economy*, 1973, *81* (2, Part 2), S279–S288, doi: 10.1086/260166.

Bertollini, Roberto, Domenico Di Lallo, Pierpaolo Mastroiacovo, and Carlo A. Perucci, "Reduction of Births in Italy after the Chernobyl Accident," *Scandinavian Journal of Work, Environment & Health*, 1990, *16* (2), 96–101, doi: 10.5271/sjweh.1803.

Black, Dan A., Natalia Kolesnikova, Seth G. Sanders, and Lowell J. Taylor, "Are Children "Normal"?," *The Review of Economics and Statistics*, 2013, *95* (1), 21–33, doi: 10.1162/REST_a_00257.

Cameron, A. Colin, Jonah B. Gelbach, and Douglas L. Miller, "Robust Inference with Multiway Clustering," *Journal of Business & Economic Statistics*, 2011, *29* (2), 238–249, doi: 10.1198/jbes.2010.07136.

Chen, Kuan-Ming, Ming-Jen Lin, and Wei-Lun Lo, "Impacts of Childhood Disability on Family: Labor, Marriage, Fertility, and Depression," *Journal of Public Economics*, 2026, 105591, DOI: 10.1016/j.jpubeco.2026.105591.

Cheung, T. Terry, Kamhon Kan, and Tzu-Ting Yang, "Parental Responses to Child Disability: Gender Differences and Relative Earnings," *Journal of Development Economics*, 2025, *174*, 103460, DOI: 10.1016/j.jdeveco.2025.103460.

Colwell, Peter F., Carolyn A. Dehring, and Nicholas A. Lash, "The Effect of Group Homes on Neighborhood Property Values," *Land Economics*, 2000, *76* (4), 615–637, DOI: 10.2307/3146956.

Conley, Timothy G., "GMM Estimation with Cross Sectional Dependence," *Journal of Econometrics*, 1999, *92* (1), 1–45, DOI: 10.1016/S0304-4076(98)00084-0.

Couture, Victor, Jonathan I. Dingel, Allison E. Green, and Jessie Handbury, "Demographic Preferences and Income Segregation," NBER Working Paper 33386, National Bureau of Economic Research, Jan. 2025, DOI: 10.3386/w33386, URL: https://www.nber.org/papers/w33386.

de la Croix, David and Aude Pommeret, "Childbearing Postponement, Its Option Value, and the Biological Clock," *Journal of Economic Theory*, 2021, *193*, 105231, DOI: 10.1016/j.jet.2021.105231.

Dettling, Lisa J. and Melissa S. Kearney, "House Prices and Birth Rates: The Impact of the Real Estate Market on the Decision to Have a Baby," *Journal of Public Economics*, 2014, *110*, 82–100, DOI: 10.1016/j.jpubeco.2013.09.009.

Doepke, Matthias, Anne Hannusch, Fabian Kindermann, and Michèle Tertilt, "The Economics of Fertility: A New Era," in *Handbook of the Economics of the Family*, ed. by Shelly Lundberg and Alessandra Voena, vol. 1, North-Holland, 2023, pp. 151–254, DOI: 10.1016/bs.hefam.2023.01.003.

Einav, Liran, Amy Finkelstein, and Petra Persson, "The Impact of a Child with Down Syndrome," NBER Working Paper 34064, National Bureau of Economic Research, July 2025, DOI: 10.3386/w34064, URL: https://www.nber.org/papers/w34064.

Ermisch, John and Fiona Steele, "Fertility Expectations and Residential Mobility in Britain," *Demographic Research*, 2016, *35* (54), 1561–1584, DOI: 10.4054/DemRes.2016.35.54.

Farber, Stephen, "Market Segmentation and the Effects on Group Homes for the Handicapped on Residential Property Values," *Urban Studies*, 1986, *23* (6), 519–525, DOI: 10.1080/00420988620080801.

Fernández, Raquel, Inés Berniell, and Milagros Onofri, "Falling Fertility: The Changing Value of Freedom, Fulfillment, and Family," NBER Working Paper 35651, National Bureau of Economic Research, Aug. 2026, doi: 10.3386/w35651, url: https://www.nber.org/papers/w35651.

Frijters, Paul, David W. Johnston, Manisha Shah, and Michael A. Shields, "To Work or Not to Work? Child Development and Maternal Labor Supply," *American Economic Journal: Applied Economics*, 2009, *1* (3), 97–110, doi: 10.1257/app.1.3.97.

Fukai, Taiyo and Takahiro Toriyabe, "Balancing Family and Career: The Effect of Public Childcare on Fertility in Japan," RIETI Discussion Paper 25-E-033, Research Institute of Economy, Trade and Industry, Apr. 2025, url: https://www.rieti.go.jp/jp/publications/dp/25e033.pdf.

Gabriel, Stuart A. and Jennifer R. Wolch, "Spillover Effects of Human Service Facilities in a Racially Segmented Housing Market," *Journal of Urban Economics*, 1984, *16* (3), 339–350, doi: 10.1016/0094-1190(84)90031-7.

Galster, George, Peter Tatian, and Kathryn Pettit, "Supportive Housing and Neighborhood Property Value Externalities," *Land Economics*, 2004, *80* (1), 33–54, doi: 10.2307/3147143.

Guerra-Cújar, María Elvira, Mounu Prem, Paul Rodríguez-Lesmes, and Juan F. Vargas, "A Peace Baby Boom? Evidence from Colombia's Peace Agreement," *Journal of Human Resources*, 2024, Published online May 8, 2024, doi: 10.3368/jhr.1222-12701R1.

Hashimoto, Masanori, "Economics of Postwar Fertility in Japan: Differentials and Trends," *Journal of Political Economy*, 1974, *82* (2, Part 2), S170–S194, doi: 10.1086/260299.

Jaeger, David A., Theodore J. Joyce, and Robert Kaestner, "A Cautionary Tale of Evaluating Identifying Assumptions: Did Reality TV Really Cause a Decline in Teenage Childbearing?," *Journal of Business & Economic Statistics*, 2020, *38* (2), 317–326, doi: 10.1080/07350015.2018.1497510.

Kearney, Melissa S. and Phillip B. Levine, "Media Influences on Social Outcomes: The Impact of MTV's 16 and Pregnant on Teen Childbearing," *American Economic Review*, 2015, *105* (12), 3597–3632, doi: 10.1257/aer.20140012.

Kearney, Melissa S. and Phillip B. Levine, "Why Is Fertility So Low in High-Income Countries?," *Journal of Economic Literature*, 2026, *64* (3), 907–949, doi: 10.1257/jel.20261786.

Kissling, Alexandra Grace, "How Individuals and Couples Make Sterilization Decisions," PhD thesis, The Ohio State University, 2020, url: https://etd.ohiolink.edu/acprod/odb_etd/ws/send_file/send?accession=osu1589291643464269&disposition=inline (visited on 09/04/2026).

Kitao, Sagiri and Kanato Nakakuni, "On the Trends of Technology, Family Formation, and Women's Time Allocation," Working paper, April 20, 2026, url: https://sagirikitao.github.io/mywebsite/KitaoNakakuni.pdf.

Kohler, Hans-Peter, "Fertility Decline as a Coordination Problem," *Journal of Development Economics*, 2000, *63* (2), 231–263, DOI: 10.1016/S0304-3878(00)00118-8.

Kondo, Ayako, "Subtle Fertility Recovery in Cohorts Who Entered the Labour Market during the Deep Recession in Japan," *Asian Population Studies*, 2026, Published online February 16, 2026, DOI: 10.1080/17441730.2026.2628719.

Kulu, Hill and Fiona Steele, "Interrelationships Between Childbearing and Housing Transitions in the Family Life Course," *Demography*, 2013, *50* (5), 1687–1714, DOI: 10.1007/s13524-013-0216-2.

Lautharte, Ildo and Imran Rasul, "The Anatomy of a Public Health Crisis: Household Responses over the Course of the Zika Epidemic in Brazil," *Journal of Health Economics*, 2026, *107*, 103126, DOI: 10.1016/j.jhealeco.2026.103126.

Li, Grace, Subhashini Chandrasekharan, and Megan Allyse, "The Top Priority Is a Healthy Baby: Narratives of Health, Disability, and Abortion in Online Pregnancy Forum Discussions in the US and China," *Journal of Genetic Counseling*, 2017, *26* (1), 32–39, DOI: 10.1007/s10897-016-9976-3.

Lovenheim, Michael F. and Kevin J. Mumford, "Do Family Wealth Shocks Affect Fertility Choices? Evidence from the Housing Market," *The Review of Economics and Statistics*, 2013, *95* (2), 464–475, DOI: 10.1162/REST_a_00266.

Lowe, Matt, "Types of Contact: A Field Experiment on Collaborative and Adversarial Caste Integration," *American Economic Review*, 2021, *111* (6), 1807–1844, DOI: 10.1257/aer.20191780.

Massenkoff, Maxim and Nathan Wilmers, "Rubbing Shoulders: Class Segregation in Daily Activities," *Journal of Public Economics*, 2025, *244*, 105335, DOI: 10.1016/j.jpubeco.2025.105335.

Miller, Grant, Áureo de Paula, and Christine Valente, "Subjective Expectations and Demand for Contraception," *Journal of Econometrics*, 2025, *249*, 105997, DOI: 10.1016/j.jeconom.2025.105997.

Ministry of Health, Labour and Welfare, "Using Disability Welfare Services under the Comprehensive Support for Persons with Disabilities Act," April 2018 edition, in Japanese, Apr. 2018, URL: https://www.mhlw.go.jp/tenji/dl/file01-01.pdf (visited on 09/04/2026).

Ministry of Health, Labour and Welfare, "Abridged Life Tables for Japan 2020," Male and female life tables, in Japanese, July 30, 2021, URL: https://www.mhlw.go.jp/toukei/saikin/hw/life/life20/ (visited on 09/07/2026).

Mizumoto, Kenji and Gerardo Chowell, "Temporary Fertility Decline after Large Rubella Outbreak, Japan," *Emerging Infectious Diseases*, 2020, *26* (6), 1122–1129, DOI: 10.3201/eid2606.181718.

Munshi, Kaivan and Jacques Myaux, "Social Norms and the Fertility Transition," *Journal of Development Economics*, 2006, *80* (1), 1–38, DOI: 10.1016/j.jdeveco.2005.01.002.

Nilforoshan, Hamed, Wenli Looi, Emma Pierson, Blanca Villanueva, Nic Fishman, Yiling Chen, John Sholar, Beth Redbird, David Grusky, and Jure Leskovec, "Human Mobility Networks Reveal Increased Segregation in Large Cities," *Nature*, 2023, *624*, 586–592, DOI: 10.1038/s41586-023-06757-3, URL: https://www.nature.com/articles/s41586-023-06757-3.

OECD, *OECD Economic Surveys: Japan 2024*, Paris: OECD Publishing, 2024, DOI: 10.1787/41e807f9-en.

Okahara, Masayuki, Shinichiro Kumagaya, and Asako Kamihigashi, "The 52nd Frontier of Social Welfare Seminar: Five Years After the Sagamihara Stabbings: Have the Lessons Been Learned?," *Rikkyo Social Work Review*, 2022, *41*, In Japanese, 33–53, DOI: 10.14992/0002001205.

Oster, Emily, "Unobservable Selection and Coefficient Stability: Theory and Evidence," *Journal of Business & Economic Statistics*, 2019, *37* (2), 187–204, DOI: 10.1080/07350015.2016.1227711.

Pettigrew, Thomas F. and Linda R. Tropp, "A Meta-Analytic Test of Intergroup Contact Theory," *Journal of Personality and Social Psychology*, 2006, *90* (5), 751–783, DOI: 10.1037/0022-3514.90.5.751.

Rangel, Marcos A., Jenna Nobles, and Amar Hamoudi, "Brazil's Missing Infants: Zika Risk Changes Reproductive Behavior," *Demography*, 2020, *57* (5), 1647–1680, DOI: 10.1007/s13524-020-00900-9.

Santos Silva, J. M. C. and Silvana Tenreyro, "The Log of Gravity," *The Review of Economics and Statistics*, 2006, *88* (4), 641–658, DOI: 10.1162/rest.88.4.641.

Skoy, Evelyn, "Household Impacts of Child Health Shocks," *Journal of Population Economics*, 2024, *37*, 20, DOI: 10.1007/s00148-024-01003-0.

Takeda, Eri, Nobuhiro Suzumori, Kyoko Kumagai, Chisato Komata, Yumiko Nishimura, and Mayumi Sugiura-Ogasawara, "Feelings and Thoughts about Life Selection in Pregnant Women Undergoing Non-Invasive Prenatal Testing in Japan," *Congenital Anomalies*, 2025, *65* (1), e12586, DOI: 10.1111/cga.12586.

Yamaguchi, Shintaro, "Effects of Parental Leave Policies on Female Career and Fertility Choices," *Quantitative Economics*, 2019, *10* (3), 1195–1232, DOI: 10.3982/QE965.

Appendix to "Possible Futures in Sight: Disability Service Facilities and Local Fertility" (Not for Publication)

A Further details on the data

This appendix provides data sources and variable-construction details for the main and supplementary analyses.

A.1 Census source files and harmonization

The 2020 Population Census used for the main analysis follow the Statistics Bureau of Japan's regional-mesh system (Statistics Bureau of Japan, 2026), which contain population by sex and five-year age group at the 250m mesh level. I download all 47 prefectural ZIP archives from e-Stat's Statistical GIS, sum prefectural component counts for mesh codes crossing prefectural borders, and retain a mesh only when every component has the ordinary-record code (`HTKSYORI=0`). This rule excludes both suppressed cells due to privacy reasons and cells receiving their aggregated counts. To avoid too small denominators of the child-to-woman ratio, the minimum of 10 women ages 15–49 is applied to the main sample before estimation.

The 2020 Census table also supplies education and residence-duration variables at 250 m resolution (Statistics Bureau of Japan, 2022a). The university-graduate share is merged to the age table by mesh code. Housing counts also come from the 2020 Census 250 m table (Statistics Bureau of Japan, 2020b). The private-car-use measure uses Statistics Bureau of Japan (2022b). Construction of the housing and private-car-use shares is described in Appendix A.4.

The 2015 cross-sectional replication and future-entry placebo use the 250m mesh data from the 2015 Population Census (Statistics Bureau of Japan, 2015a; Statistics Bureau of Japan, 2015b). Housing shares apply the 2020 definitions to 2015 household counts. A comparable university-graduate share is unavailable, so the 2015 regressions do not use it as a control variable.

To obtain changes in the female population, I merge the 2020 mesh data to the 2015 mesh data by identical mesh codes (Statistics Bureau of Japan, 2025; Statistics Bureau of Japan, 2015a).[A.1] The child cohort measures in Appendix A.7 also require merging the 2015 and 2020 mesh data (Statistics Bureau of Japan, 2015a; Statistics Bureau of Japan, 2020a). The measure for ages 5–9 in 2020 pairs the 2015 population ages 0–4 with the 2020 population ages 5–9; the measure for ages 10–14 in 2020 pairs ages 5–9 in 2015 with ages 10–14 in 2020. The female recent-mover share uses the sex-specific residence-duration items in the 2020 data.

A.2 Facility definitions and spatial sample

To obtain the location of welfare facilities, I use the 2021 National Land Numerical Information Welfare Facilities Data (Ministry of Land, Infrastructure, Transport and Tourism, 2021). I retain point coordinates, facility names, classification codes, and positional accuracy. After

[A.1] There is a very slight modification of the coordinate system from the 2015 mesh data (JGD2000) to the 2020 mesh data (JGD2011). I ignore this difference in merging the two datasets.

removing duplicates defined by location, municipality code, name, and minor classification, the file contains 266,572 points. Positional accuracy codes 1 and 2 account for 265,781 points; 783 code-3 points and eight code-4 points are excluded before any spatial operation because of its inprecise location data. Accuracy code 2 can identify a koaza or block representative location rather than an exact building, but it fairly accurately identifies the location. Code 1 is the exact identification at the building level.

The data contain the classification of welfare facilities, based on the major codes, middle codes, and the minor code.[A.2] Adult disability service facilities include all records in major code 03, disability support facilities and related establishments (障害者支援施設等); major code 04, facilities supporting the social participation of people with physical disabilities (身体障害者社会参加支援施設); or middle code 9911, disability service facilities (障害者サービス施設). Code 03 covers disability support facilities, community activity support centers, and welfare homes. Code 04 covers physical-disability welfare centers, rehabilitation and recreation centers, assistive-device production facilities, guide-dog training facilities, and information facilities for people with visual or hearing disabilities. Within these codes, all subordinate, other, and unspecified categories are retained. This leaves me with 58,044 adult disability service facility points.

The main definition excludes middle codes 0508, residential facilities for children with disabilities (障害児入所施設), and 0509, child development support centers (児童発達支援センター) because they may be directly relevant for childraising through providing some childcare amenities or other public goods. The sensitivity analysis below adds these two child-service categories to the adult-service definition in Section 3. Adding 443 admissible points in code 0508 and 4,069 in code 0509 expands the facility universe to 62,267 points. Reconstructing nearest-facility assignments, facility-cell exclusions, and common fixed-effect support for the same three specifications yields 193,144 cells instead of 190,747. In the same specification of Column 3 of Table 1, the 0–250 m coefficient is −6.73 (standard error 3.13, $p = 0.031$), compared with −7.39 in the main analysis. The nearest-band association remains negative and significant at the 5 percent level.

The elderly care facility placebo includes all records in major code 02, welfare facilities for older people (老人福祉施設), or middle codes 9907, fee-based homes for older people (有料老人ホーム); 9908, recreation facilities for older people (老人憩の家); and 9910, long-term-care insurance and related facilities (介護保険等の施設). Code 02 covers residential homes, welfare and day-service centers, short-stay facilities, home-care support, and supported living, including other and unspecified subcategories. Code 9907 includes service-equipped housing classified as a fee-based home. Code 9910 covers nursing homes, long-term-care welfare and health facilities, medical and integrated care institutions, and other care services. The same positional-accuracy restriction leaves 130,545 points.

[A.2] Official classification lists: major codes, middle codes, and minor codes.

A.3 Summary statistics

Table A.1 reports statistics weighted by women ages 15–49 for the 190,747-cell common sample defined in Section 3.

Table A.1: Summary Statistics for the Main Estimation Sample

Variable	Mean	SD	p25	p50	p75	*N*
A. Outcome, exposure, and population						
Child–woman ratio	191.86	99.69	127.27	176.47	237.41	190,747
Distance to nearest facility (km)	0.491	0.293	0.271	0.408	0.628	190,747
Total population	645.01	511.92	296	508	843	190,747
Women ages 15–49	141.32	129.32	58	104	180	190,747
Children ages 0–4	26.86	31.95	9	19	33	190,747
B. Baseline controls						
ln(population density)	8.909	0.787	8.418	8.956	9.460	190,747
Population ages 65+ (%)	24.04	9.99	17.16	23.25	30.27	190,747
Mean age of women ages 15–49	33.90	1.76	33.01	33.94	34.91	190,747
University-graduate share (%)	25.50	11.33	16.96	23.89	32.82	190,747
Residential zoning indicator	0.689	0.463	0	1	1	190,747
Commercial zoning indicator	0.076	0.265	0	0	0	190,747
Industrial zoning indicator	0.086	0.280	0	0	0	190,747
Row-house share (%)	1.49	3.81	0.00	0.24	1.54	190,747
Apartment share (%)	46.16	30.02	20.55	45.11	71.47	190,747
Other/unstated housing share (%)	0.09	0.55	0.00	0.00	0.00	190,747

Notes: Statistics describe 250 m cells in the main estimation sample. Means, standard deviations (SD), and percentiles are weighted by the number of women ages 15–49; *N* counts cells. The p25, p50, and p75 columns show the weighted 25th, 50th, and 75th percentiles. The CWR is children ages 0–4 per 1,000 women ages 15–49. Population density is residents per square kilometer before taking logs. Shares are percentages, and zoning indicators are zero or one. Housing shares use households living in housing as the denominator.

A.4 Baseline controls and private-car use

Population density is total population divided by the spherical area of the 250 m cell and enters the baseline vector as $\ln(\text{density})$. The share age 65 or older divides the population in this age group by total population. Mean age among women ages 15–49 is approximated by weighting the midpoints 17, 22, 27, 32, 37, 42, and 47 by the corresponding five-year female age-group counts.

The university-graduate share divides university and graduate-school graduates ages 15 or older by all final-school graduates ages 15 or older, pooling men and women. I use the published graduate total without subtracting cases with an unreported final school. Housing shares use all general households living in housing as the denominator. Row-house and apartment counts come directly from the table; other or unstated forms are the residual after subtracting detached houses, row houses, and apartments. Detached houses form the omitted category.

Zoning is constructed from the 2019 National Land Numerical Information (Ministry of Land, Infrastructure, Transport and Tourism, 2019). Each 250m cell centroid is spatially joined to the zoning GIS data. Zoning codes 1–7 and 21 are classified as residential, 8–9 as commercial, and 10–12 as industrial. All three indicators equal zero for other designated zones and for cells without zoning, which together form the omitted category.

The private-car-use measure is constructed from the 2020 Census 250m table. I aggregate the published counts from constituent 250 m cells to each parent 500m mesh before applying estimation-sample restrictions. The rate divides private-car users commuting to work or school by resident workers and students excluding people working at home. I assign the parent rate to each constituent cell. Respondents report every commuting mode used, so the rate measures any private-car use rather than car-only commuting (Statistics Bureau of Japan, 2020c).

A.5 Transit data and walking-network construction

Using the 2020 railway data (Ministry of Land, Infrastructure, Transport and Tourism, 2020c), I average the vertices of each station feature and collapse co-located points, leaving 9,723 unique station points. I also use the 2022 bus-stop data (Ministry of Land, Infrastructure, Transport and Tourism, 2022), which yield 242,984 unique coordinate points after duplicate locations are collapsed. Each admissible adult disability facility is assigned its nearest station and nearest bus stop by great-circle distance.

Walking paths are traced on the January 1, 2021 historical OpenStreetMap network for Japan, supplied in eight Geofabrik regional extracts (OpenStreetMap contributors, 2021), using the GraphHopper 11.0 foot profile (GraphHopper, 2026). I compute paths from each facility to its nearest station and bus stop. Placebo paths use the same procedure after rotating the straight facility-to-destination vector by 90, 180, or 270 degrees in local east–north coordinates. This preserves the facility anchor and straight-line endpoint distance, while routed lengths can change. For each direction, a cell's pooled indicator is one if its rectangle intersects either available path assigned to its nearest facility, zero if paths are available but neither intersects the cell, and missing if neither path is available.

The facility and destination coordinates may lie off the mapped walking network, especially when the destination is a rotated placebo endpoint. GraphHopper connects each coordinate to the nearest road segment accessible to pedestrians. This connection is called a "snap." I retain a path only if routing succeeds and the distance from each endpoint to its network connection point is no greater than 2 km. This threshold applies separately to the connections at the two endpoints, rather than to the total path length. Among retained placebo paths, the distance from the rotated endpoint to the network has a median of 16.6 m and a 99th percentile of 377 m.

When determining whether a path intersects a cell, I include the route along the walking network and the straight connectors between the original endpoint coordinates and the network. A cell therefore counts as intersecting the path if either the network route or a connector intersects its rectangle.

For the pooled analysis, which is my main specification in Section 4.2.1, I combine the station-derived and bus-derived paths separately for each of the four directions: the actual direction and the three placebo rotations. Each cell is evaluated using the paths associated with its nearest facility. The pooled indicator equals one if either available path intersects the cell. It equals zero if at least one path is available but no available path intersects the cell, and is missing only if neither path is available. Thus, both destination types need not be available in a given direction. Of the 26,220 facilities, 26,174 have at least one usable station-derived or bus-derived path at each of the three placebo rotations. The regression specification in Section 4.2.1 requires all four indicators to be nonmissing. I then apply the fixed-effect support restrictions: cells that are the only remaining observation assigned to a facility or within a parent 500 m mesh are removed, and this process is repeated until no such cells remain. The resulting estimation sample contains 190,445 cells.

The station-only and bus-only regressions in Appendix Tables B.3 and B.4 require, for comparability between bus and train stations, all four station-derived paths and all four bus-derived paths to be available. After the same support restrictions, both regressions use the same 182,873 cells, so differences between their estimates do not reflect differences in sample composition. Each regression includes only its own destination type's four indicators.

A.6 New-entrant facilities and the 2015 analyses

The future-entry placebo screens individual adult disability facility records observed in 2021 against the two older (2011 and 2015) versions of the same welfare-facility datasets (Ministry of Land, Infrastructure, Transport and Tourism, 2011; Ministry of Land, Infrastructure, Transport and Tourism, 2015; Ministry of Land, Infrastructure, Transport and Tourism, 2021). I retain 2021 records with positional-accuracy codes 1 or 2 and use each record's original coordinates. Because the 2015 facility dataset does not cover Osaka, I exclude both facility records and

Census cells in Osaka. The resulting universe contains 52,225 accurately located adult disability facility records.

For each 2021 facility, I check whether any welfare facility was recorded within 250m of its location in either 2011 or 2015. If so, I exclude it from the placebo candidates. To avoid influence of any type of welfare facility, this check includes elderly and child welfare facilities, as well as disability facilities. I then compare each facility's name and address with the 2011 and 2015 records and exclude it if an earlier record in the same prefecture has the same name or address within 5km, or a very similar name within 2km. I use both the 2011 and 2015 data to safeguard against the measurement error such as temporal closure or reallocation. This procedure leaves 10,026 future entrants of the disability service facilities.

The cross-sectional replication using the 2015 data measures proximity to individual adult disability service facilities recorded in Ministry of Land, Infrastructure, Transport and Tourism (2015). I apply the 2015 fine-classification codes to retain adult disability services, excluding child-only, public-assistance, and generic categories whose adult-disability eligibility cannot be established. After removing duplicate records with identical prefecture, coordinates, fine classification, name, and address, I retain 29,030 eligible records at their original coordinates. Nearby records remain separate, and their locations are not averaged. Osaka is omitted because its 2015 facility dataset is unavailable.

A.7 Residential sorting and migration measures

Four measures of the residential sorting and migration in Section 4.3.2 are constructed as follows.

For children, let $C_{it}^{a\text{–}b}$ denote the number of children ages a through b in cell i in year t. Net child migration rate (5–9 as of 2020) is defined as

$$S_i^{C,1} = 100\left(\frac{C_{i,2020}^{5\text{–}9}}{C_{i,2015}^{0\text{–}4}} - 1\right), \qquad C_{i,2015}^{0\text{–}4} > 0. \tag{A.1}$$

Net child migration rate (10–14 as of 2020) follows the next older cohort:

$$S_i^{C,2} = 100\left(\frac{C_{i,2020}^{10\text{–}14}}{C_{i,2015}^{5\text{–}9}} - 1\right), \qquad C_{i,2015}^{5\text{–}9} > 0. \tag{A.2}$$

A rate of zero indicates unchanged cohort population. Positive and negative values proxy net inflows and outflows as a percentage of the 2015 cohort, apart from mortality. I ignore the mortality and interpret it as the net migration measure given the very low child mortality rate in Japan.

Let W_{it} denote the number of women ages 15–49 in cell i in Census year t. Their population change is defined as

$$G_i^W = 100 \left[\ln W_{i,2020} - \ln W_{i,2015}\right]. \tag{A.3}$$

Both counts are strictly positive in my sample. Regressions with G_i^W as the outcome use $(W_{i,2020} + W_{i,2015})/2$ as the analytic weight.

The female recent-mover share is

$$R_i^W = 100 \times \frac{F_{i,<1\text{ year}} + F_{i,1\text{–}5\text{ years}}}{F_{i,\text{birth}} + F_{i,<1\text{ year}} + F_{i,1\text{–}5\text{ years}} + F_{i,5\text{–}10\text{ years}} + F_{i,10\text{–}20\text{ years}} + F_{i,20+\text{ years}}}, \tag{A.4}$$

where the categories cover female residents of all ages in 2020 with known duration at their current address.[A.3] An unknown duration is excluded from the denominator. The share captures recent moves among current residents.

A.8 Residential land-price measures

The residential land-price measure pools the 2020 Land Price Publication, assessed on January 1, and Prefectural Land Price Survey (L02), assessed on July 1 (Ministry of Land, Infrastructure, Transport and Tourism, 2020a; Ministry of Land, Infrastructure, Transport and Tourism, 2020b). I retain points whose recorded current use is exclusively residential and predict the natural logarithm of land price in yen per square meter at each 250 m cell centroid using the two nearest points, weighting their log prices by inverse squared distance. The median distance to the second point is 0.76 km in the main sample. Appendix B.5 describes its use as a control and an outcome.

A.9 Recorded-crime sources and geographic matching

The nationwide theft database was compiled and geocoded by Mamoru Amemiya and collaborators from prefectural-police open data (Amemiya and Yamane, 2021; Amemiya and Tanaka, 2022). Its seven theft categories are purse snatching, theft from vehicles, vehicle-parts theft, vending-machine theft, motor-vehicle theft, motorcycle theft, and bicycle theft. The 2019 and 2020 files contain 249,272 and 180,646 records, respectively, and are distributed under CC BY 4.0 through the University of Tsukuba's Division of Policy and Planning Sciences Commons Data Bank.

The compilers match police-reported town/chome or oaza addresses to representative coordinates, rather than exact crime locations. Records without a neighborhood may be imputed only at the municipality or prefecture level using police-jurisdiction information. Retaining records with valid coordinates and a reported neighborhood leaves 248,067 records in 2019 and 179,194 in 2020, respectively 99.52 and 99.20 percent of the source files. Retained records are

[A.3] $F_{i,\text{birth}}$ means those who live in the current location since their birth. Analogously, other variables indicate the number of people who have spent x years in the current residence.

assigned to 250 m meshes by their coordinates and counted by year and theft category. Annual theft rates divide these counts by 2020 cell population and multiply by 1,000; the 2019–2020 outcome is the mean of the two annual rates. Both nationwide theft-outcome regressions and CWR regressions controlling for theft require at least 50 residents per 250 m cell. Recursive removal of facility and parent-500 m singletons then yields the common 185,995-cell sample.

The second source is the Tokyo Metropolitan Police Department's annual town/chome crime table for 2019–2021 (Tokyo Metropolitan Police Department, 2026). Normalized place names are matched to 2020 Census small-area boundaries, populations, and representative points from e-Stat (Statistics Bureau of Japan, 2020d). These data include all recorded Penal Code offenses and allow separate outcomes for violent or serious offenses, burglary, and non-burglary theft. Tokyo crime rates use 2020 population and are expressed per 1,000 residents. Eligible town/chome areas have at least 50 residents, positive area with no upper limit, and a representative point less than 1.5 km from the nearest facility. Areas containing an admissible adult disability facility are excluded. The fixed-effect specifications may retain different subsets after singleton removal.

A.10 Alternative CWR denominator

The alternative CWR retains the age-0–4 numerator in Equation (1) and restricts the denominator to women ages 20–39:

$$\mathrm{CWR}_i^{20\text{–}39} = 1000 \times \frac{\text{children ages 0–4}_i}{\text{women ages 20–39}_i}. \tag{A.5}$$

Table B.15 compares the two CWR definitions on a common sample with at least 10 women ages 20–39 and the required fixed-effect support. Each regression uses its own female-population denominator as the analytic weight.

B Supplementary analyses

This appendix follows the analyses in the main text. Appendix A documents sources and variable construction.

Unless stated otherwise, regressions follow Equation (2): five 250 m distance bands are compared with 1.25–1.50 km, facility-containing cells are excluded for the relevant facility type, and weights are the number of women ages 15–49. Column (1) includes nearest-facility fixed effects and clusters by facility; column (2) adds parent-500 m fixed effects and two-way clustering; column (3) adds the ten baseline controls. Each analysis uses a common complete-case sample after recursively removing fixed-effect singletons.

B.1 Transit-route direction and alternative paths

The route analysis in Section 4.2.1 examines opportunities for incidental social contact by adding four path indicators to each main specification: the actual transit path and three rotated placebo paths. Appendix A.5 describes their construction.

Table B.1 uses 190,445 cells with all four pooled indicators available under the rule in Appendix A.5. Figure 4 displays the column-(3) route coefficients.

The directional contrast compares the actual-path coefficient with the mean of the three rotated-path coefficients from the same joint regression:

$$\begin{aligned} \Delta_R &= \theta_A - \frac{\theta_{90} + \theta_{180} + \theta_{270}}{3}, \\ \widehat{\mathrm{se}}(\widehat{\Delta}_R) &= \sqrt{\ell' \widehat{V}_\theta \ell}, \end{aligned} \tag{B.1}$$

where $\ell = (1, -1/3, -1/3, -1/3)'$ and $\widehat{V}_\theta$ is the full clustered covariance submatrix of the four route coefficients in that order. The contrast compares the actual path with the average rotated path, not each pair separately.

Table B.1: Distance Bands with OSM-Routed Actual and Rotated Transit Paths

Variable	(1)	(2)	(3)
Distance to nearest disability facility			
0–0.25 km	−4.662**	−6.772*	−6.940**
	(2.171)	(3.572)	(3.341)
0.25–0.50 km	−1.718	−5.186	−6.199**
	(1.931)	(3.317)	(3.105)
0.50–0.75 km	−0.449	−5.391*	−6.325**
	(1.898)	(3.194)	(2.975)
0.75–1.00 km	1.222	−2.760	−3.842
	(1.907)	(2.900)	(2.699)
1.00–1.25 km	−0.754	−2.607	−2.520
	(1.916)	(2.225)	(2.120)
1.25–1.50 km (reference)	0	0	0
OSM-routed path indicators entered jointly			
Actual station-or-bus path	−4.963***	−3.373***	−2.798***
	(0.798)	(1.004)	(0.934)
Path to endpoint rotated 90 degrees	−0.346	0.256	0.787
	(0.771)	(0.965)	(0.893)
Path to endpoint rotated 180 degrees	2.333***	1.525	1.828**
	(0.807)	(0.972)	(0.896)
Path to endpoint rotated 270 degrees	0.119	−0.720	−0.764
	(0.800)	(0.949)	(0.880)
Actual − mean of rotated paths	−5.665***	−3.727***	−3.415***
	(0.948)	(1.182)	(1.098)
Facility fixed effects	Yes	Yes	Yes
Parent-500 m fixed effects	No	Yes	Yes
Baseline controls	No	No	Yes
Observations	190,445	190,445	190,445

Notes: The outcome is the 2020 CWR (children ages 0–4 per 1,000 women ages 15–49); the reference band is 1.25–1.50 km. Indicators mark cells intersected by walking paths from their nearest facility. Station and bus paths are combined, with at least one available in each direction. The actual path and the three paths to rotated endpoints enter jointly (Appendix A.5). All columns use the same sample, exclude cells containing adult disability facilities, and weight by women ages 15–49. Controls follow Table 1. Standard errors in parentheses cluster by facility in column (1) and by facility and parent-500 m mesh in columns (2)–(3). $^{*}p < 0.10$, $^{**}p < 0.05$, $^{***}p < 0.01$.

Geometric straight-line corridors. Table B.2 replaces network paths in Equation (3) with direct facility-to-station and facility-to-bus-stop segments and their 90-, 180-, and 270-degree rotations. These indicators approximate route direction without imposing a walkable street network.

Table B.2: Geometric Straight-Line Transit Corridors and Rotated Placebos

Variable	(1)	(2)	(3)
Distance to nearest disability facility			
0–0.25 km	-5.624^{**}	-6.672^{*}	-6.270^{*}
	(2.188)	(3.586)	(3.349)
0.25–0.50 km	-2.125	-5.234	-6.045^{*}
	(1.926)	(3.312)	(3.098)
0.50–0.75 km	-0.636	-5.431^{*}	-6.276^{**}
	(1.896)	(3.189)	(2.969)
0.75–1.00 km	1.102	-2.805	-3.833
	(1.906)	(2.896)	(2.694)
1.00–1.25 km	-0.798	-2.640	-2.550
	(1.914)	(2.222)	(2.118)
1.25–1.50 km (reference)	0	0	0
Geometric corridor indicators entered jointly			
Actual station-or-bus corridor	-4.032^{***}	-2.772^{***}	-2.093^{**}
	(0.831)	(1.018)	(0.957)
Corridor rotated 90 degrees	-0.217	-0.835	-0.888
	(0.825)	(0.988)	(0.919)
Corridor rotated 180 degrees	2.530^{***}	1.340	1.232
	(0.853)	(1.024)	(0.945)
Corridor rotated 270 degrees	0.236	-0.673	-0.808
	(0.854)	(1.016)	(0.947)
Actual − mean of rotated paths	-4.881^{***}	-2.716^{**}	-1.938^{*}
	(0.891)	(1.123)	(1.063)
Facility fixed effects	Yes	Yes	Yes
Parent-500 m fixed effects	No	Yes	Yes
Baseline controls	No	No	Yes
Observations	190,747	190,747	190,747

Notes: The outcome is the 2020 CWR (children ages 0–4 per 1,000 women ages 15–49); the reference band is 1.25–1.50 km. Indicators mark cells intersected by straight lines from their nearest facility to its nearest station or bus stop. Both destination types are combined. The actual lines and their 90-, 180-, and 270-degree rotations enter jointly. All columns use the same sample, exclude cells containing adult disability facilities, and weight by women ages 15–49. Controls follow Table 1. Standard errors in parentheses cluster by facility in column (1) and by facility and parent-500 m mesh in columns (2)–(3). $^{*}p < 0.10$, $^{**}p < 0.05$, $^{***}p < 0.01$.

Tables B.3 and B.4 replace the pooled station-or-bus path indicators in Equation (3) with station-only and bus-only path indicators, respectively. Each regression includes the selected destination type's four indicators. Both use the same 182,873 cells with all eight component paths available, as documented in Appendix A.5.

Table B.3: Station-Only OSM Transit Paths

Variable	(1)	(2)	(3)
Distance to nearest disability facility			
0–0.25 km	-5.201^{**}	-7.143^{**}	-7.125^{**}
	(2.132)	(3.596)	(3.361)
0.25–0.50 km	-1.898	-5.059	-6.048^{*}
	(1.953)	(3.380)	(3.164)
0.50–0.75 km	-0.478	-5.118	-6.139^{**}
	(1.932)	(3.260)	(3.037)
0.75–1.00 km	0.884	-2.880	-3.909
	(1.934)	(2.963)	(2.755)
1.00–1.25 km	-0.662	-2.565	-2.382
	(1.954)	(2.265)	(2.159)
1.25–1.50 km (reference)	0	0	0
OSM-routed path indicators entered jointly			
Actual station path	-4.336^{***}	-2.920^{***}	-2.627^{***}
	(0.846)	(1.075)	(1.006)
Path to endpoint rotated 90 degrees	0.156	0.593	1.348
	(0.845)	(1.059)	(0.984)
Path to endpoint rotated 180 degrees	1.753^{**}	1.472	1.853^{*}
	(0.882)	(1.048)	(0.960)
Path to endpoint rotated 270 degrees	-0.112	-1.288	-1.178
	(0.855)	(1.040)	(0.962)
Actual − mean of rotated paths	-4.935^{***}	-3.179^{**}	-3.301^{***}
	(0.994)	(1.251)	(1.172)
Facility fixed effects	Yes	Yes	Yes
Parent-500 m fixed effects	No	Yes	Yes
Baseline controls	No	No	Yes
Observations	182,873	182,873	182,873

Notes: The outcome is the 2020 CWR (children ages 0–4 per 1,000 women ages 15–49); the reference band is 1.25–1.50 km. Indicators mark cells intersected by walking paths from their nearest facility to its nearest station or to three rotated endpoints. All four enter jointly (Appendix A.5). This table and Table B.4 use the same cells with all eight station and bus paths available. All columns exclude cells containing adult disability facilities and weight by women ages 15–49. Controls follow Table 1. Standard errors in parentheses cluster by facility in column (1) and by facility and parent-500 m mesh in columns (2)–(3). $^{*}p < 0.10$, $^{**}p < 0.05$, $^{***}p < 0.01$.

Table B.4: Bus-Only OSM Transit Paths

Variable	(1)	(2)	(3)
Distance to nearest disability facility			
0–0.25 km	−5.183**	−7.031*	−6.572*
	(2.148)	(3.637)	(3.399)
0.25–0.50 km	−2.112	−5.157	−5.960*
	(1.937)	(3.374)	(3.158)
0.50–0.75 km	−0.642	−5.191	−6.120**
	(1.928)	(3.258)	(3.034)
0.75–1.00 km	0.791	−2.931	−3.913
	(1.934)	(2.963)	(2.754)
1.00–1.25 km	−0.707	−2.594	−2.390
	(1.954)	(2.265)	(2.159)
1.25–1.50 km (reference)	0	0	0
OSM-routed path indicators entered jointly			
Actual bus stop path	−3.722***	−2.474*	−1.135
	(1.106)	(1.324)	(1.228)
Path to endpoint rotated 90 degrees	−2.041*	−1.104	−1.226
	(1.045)	(1.291)	(1.199)
Path to endpoint rotated 180 degrees	1.557	0.141	−0.086
	(1.074)	(1.305)	(1.215)
Path to endpoint rotated 270 degrees	1.194	1.059	0.515
	(1.151)	(1.315)	(1.206)
Actual − mean of rotated paths	−3.959***	−2.507	−0.869
	(1.313)	(1.587)	(1.463)
Facility fixed effects	Yes	Yes	Yes
Parent-500 m fixed effects	No	Yes	Yes
Baseline controls	No	No	Yes
Observations	182,873	182,873	182,873

Notes: The outcome is the 2020 CWR (children ages 0–4 per 1,000 women ages 15–49); the reference band is 1.25–1.50 km. Indicators mark cells intersected by walking paths from their nearest facility to its nearest bus stop or to three rotated endpoints. All four enter jointly (Appendix A.5). This table and Table B.3 use the same cells with all eight station and bus paths available. All columns exclude cells containing adult disability facilities and weight by women ages 15–49. Controls follow Table 1. Standard errors in parentheses cluster by facility in column (1) and by facility and parent-500 m mesh in columns (2)–(3). $^{*}p < 0.10$, $^{**}p < 0.05$, $^{***}p < 0.01$.

B.2 Private-car-use heterogeneity

Figure 5 shows how the proximity association varies with private-car use, which may limit opportunities for incidental social contact. The flexible model estimates a separate car-use interaction for each of the five included distance bands and retains unrestricted distance-band main effects.

Let $c_{m(i)}$ be the share of commuters and students using private cars in cell i's parent-500 m mesh, expressed between zero and one. Define

$$z_{m(i)} = \frac{c_{m(i)} - \bar{c}_w}{0.10}, \qquad \bar{c}_w \simeq 0.42982,$$

where $\bar{c}_w$ is the women-weighted mean: $z_{m(i)} = 0$ at mean car use, and one unit represents 10 percentage points. The indicator D_{ib} identifies distance band b, from $b = 0$ (0–250 m) through $b = 4$ (1.00–1.25 km), with 1.25–1.50 km omitted. The equation below gives the preferred specification:

$$\begin{aligned} \mathrm{CWR}_i = {} & \sum_{b=0}^{4} \beta_b D_{ib} + \sum_{b=0}^{4} \theta_b z_{m(i)} D_{ib} \\ & + X_i' \gamma + \alpha_{f(i)} + \delta_{m(i)} + u_i. \end{aligned} \tag{B.2}$$

The coefficient θ_b measures the change per 10 percentage points of car use in band b relative to the omitted band. At rate c, the CWR difference is $\beta_b + \theta_b(c - \bar{c}_w)/0.10$. This model estimates five interaction coefficients freely, allowing their signs and magnitudes to vary across bands.

The preferred specification uses 190,747 cells, nearest-facility and parent-500 m fixed effects, and the ten baseline controls. Parent-500 m fixed effects absorb the car-use level, while the interactions remain estimable because distance can vary among constituent 250 m cells.

Figure 5 in the main text evaluates this specification at the women-weighted 10th, 50th, and 90th percentiles of car use (8.5, 41.5, and 79.1 percent). All three profiles use Equation (B.2), with 95 percent confidence intervals calculated from the full clustered covariance matrix.

B.3 Placebo analyses and 2015 cross-sectional replication

B.3.1 Future entry of disability facilities placebo

This placebo checks whether the 2015 CWR was already lower near candidate future disability facilities observed in 2021. The candidates pass the 2011 and 2015 historical screens described in Appendix A.6.

I repeat the main distance-band specifications using the 2015 CWR and weights based on women ages 15–49 in 2015, excluding cells containing candidates. Column (3) uses nine controls rather than ten because a comparable 2015 university-graduate share is unavailable. Other estimation conventions follow the introduction to this appendix. Table B.5 reports the estimates for the common 138,229-cell sample shown in Panel A of Figure 6. The estimates provide no clear evidence of lower CWR near these candidates in 2015.

Table B.5: Future Entry of Disability Facilities Placebo: 2015 CWR

Distance band (km)	(1)	(2)	(3)
0–0.25	−0.587	0.892	0.105
	(1.640)	(2.615)	(2.411)
0.25–0.50	0.799	1.262	1.071
	(1.381)	(2.313)	(2.116)
0.50–0.75	0.961	0.060	0.271
	(1.306)	(2.076)	(1.916)
0.75–1.00	0.698	−0.553	−0.478
	(1.240)	(1.810)	(1.646)
1.00–1.25	0.362	−0.629	−0.001
	(1.167)	(1.385)	(1.260)
1.25–1.50 (reference)	0	0	0
Facility fixed effects	Yes	Yes	Yes
Parent-500 m fixed effects	No	Yes	Yes
Nine controls	No	No	Yes
Observations	138,229	138,229	138,229
Facilities with assigned cells	7,411	7,411	7,411

Notes: The outcome is the 2015 CWR (children ages 0–4 per 1,000 women ages 15–49); the reference band is 1.25–1.50 km. Candidates exclude 2021 adult disability facilities within 250 m of a welfare facility recorded in 2011 or 2015, or with a matching historical name or address (Appendix A.6). Osaka is excluded. All columns use the same sample and weight by women ages 15–49 in 2015. Cells containing candidates are excluded; other facility cells remain eligible. Column (3) uses nine controls, omitting the unavailable 2015 university-graduate share. Standard errors in parentheses cluster by nearest candidate facility in column (1) and by that facility and parent-500 m mesh in columns (2)–(3). $^{*}p < 0.10$, $^{**}p < 0.05$, $^{***}p < 0.01$.

B.3.2 2015 cross-sectional replication

The historical replication uses the 2015 CWR and distances to individual adult disability facility records in P14-2015, evaluated at their original coordinates. Nearest-facility assignment follows the same method as the 2020 analysis. All three columns share the sample with complete data for the nine controls and support for both fixed effects, use 2015 counts of women ages 15–49 as weights, and exclude cells containing any eligible 2015 facility record. The nearest record's ID defines the facility fixed effects and clustering groups. Appendix A.6 gives the year-specific facility definition and geographic correction.

Table B.6 reports the profiles on the common 173,854-cell sample. The corresponding 2020 estimates appear in Table 1; each year retains its own sample and facility definitions.[B.1]

Table B.6: 2015 Cross-Sectional Replication: Distance to Disability Facilities

Distance band (km)	(1)	(2)	(3)
0–0.25	−11.095***	−6.932**	−5.017*
	(1.616)	(2.780)	(2.571)
0.25–0.50	−8.289***	−6.063**	−4.373*
	(1.466)	(2.535)	(2.345)
0.50–0.75	−4.199***	−2.895	−1.554
	(1.431)	(2.356)	(2.183)
0.75–1.00	−1.510	−0.746	−0.334
	(1.389)	(2.088)	(1.946)
1.00–1.25	−2.535*	−1.725	−1.092
	(1.336)	(1.626)	(1.507)
1.25–1.50 (reference)	0	0	0
Facility fixed effects	Yes	Yes	Yes
Parent-500 m fixed effects	No	Yes	Yes
Nine controls	No	No	Yes
Observations	173,854	173,854	173,854
Facilities with assigned cells	14,714	14,714	14,714

Notes: The outcome is the 2015 CWR (children ages 0–4 per 1,000 women ages 15–49); the reference band is 1.25–1.50 km. Distances use disability facilities recorded in 2015. Osaka is excluded because its facility data are unavailable. All columns use the same sample, exclude cells containing these facilities, and weight by women ages 15–49 in 2015. Column (3) uses nine controls: three demographic measures, three housing shares, and three zoning indicators. A comparable 2015 university-graduate share is unavailable. Appendix A.6 describes the facility records. Standard errors in parentheses cluster by nearest facility in column (1) and by facility and parent-500 m mesh in columns (2)–(3). $^{*}p < 0.10$, $^{**}p < 0.05$, $^{***}p < 0.01$.

[B.1] Note that the 2015 analysis excludes Osaka due to data availability. Excluding Osaka in the 2020 analysis also makes the column-(3) 0–250 m coefficient modestly less negative, from −7.39 to −6.11.

B.3.3 Elderly care facility placebo

Table B.7 gives the 192,156-cell regressions underlying Panel B of Figure 6. Distances, facility-containing-cell exclusions, and fixed-effect groups are reconstructed for the elderly care facility universe defined in Appendix A.2; the remaining conventions are unchanged.

Table B.7: Distance to the Nearest Elderly Care Facility: Placebo Specifications

Distance band (km)	(1)	(2)	(3)
0–0.25	2.075	−0.560	2.087
	(2.547)	(3.921)	(3.787)
0.25–0.50	0.935	−1.857	0.161
	(2.480)	(3.820)	(3.701)
0.50–0.75	1.513	−0.134	1.300
	(2.455)	(3.703)	(3.593)
0.75–1.00	0.479	−2.346	−0.773
	(2.455)	(3.357)	(3.311)
1.00–1.25	−0.332	−4.725*	−2.928
	(2.376)	(2.688)	(2.700)
1.25–1.50 (reference)	0	0	0
Facility fixed effects	Yes	Yes	Yes
Parent-500 m fixed effects	No	Yes	Yes
Baseline controls	No	No	Yes
Observations	192,156	192,156	192,156

Notes: The outcome is the 2020 CWR (children ages 0–4 per 1,000 women ages 15–49); the reference band is 1.25–1.50 km. Distances and facility groups use elderly care facilities, and cells containing these facilities are excluded. All columns use the same sample and weight by women ages 15–49. Column (3) adds the baseline controls in Table 1. Standard errors in parentheses cluster by nearest elderly care facility in column (1) and by that facility and parent-500 m mesh in columns (2)–(3). $^{*}p < 0.10$, $^{**}p < 0.05$, $^{***}p < 0.01$.

B.4 Residential sorting and population outcomes

Table B.8 holds fixed a sample of 173,438 cells with positive 2015 denominators for both child cohorts, all four sorting measures observed, complete baseline variables, and support for both fixed effects. Appendix A.7 defines the measures.

Panel A compares CWR regressions with the net child migration rate for ages 5–9 in 2020 alone, both net child migration rates, and both rates plus female population change and the female recent-mover share. The specification with both rates also appears in Panel A of Table 2.

Panel B uses each sorting measure as the outcome without adding the others as controls. The net child migration rates for ages 5–9 and 10–14 in 2020 are weighted by the corresponding 2015 child populations ages 0–4 and 5–9; female population change by the average number of women ages 15–49 in 2015 and 2020; and the female recent-mover share by women with a reported residence-duration category. The migration-rate and recent-mover-share coefficients are percentage-point differences; the female-population-change coefficients are differences in 100 times log growth.

Table B.8: Residential Sorting, Population Change, and Net Child Migration

Model or outcome	(1)	(2)	(3)
Panel A: CWR outcome			
No migration controls	-5.783^{***}	-8.535^{**}	-8.052^{**}
	(2.004)	(3.493)	(3.280)
Add net child migration rate (5–9 as of 2020)	-4.768^{**}	-7.039^{**}	-6.951^{**}
	(1.979)	(3.468)	(3.250)
Add both net child migration rates	-4.766^{**}	-7.020^{**}	-7.002^{**}
	(1.980)	(3.470)	(3.251)
Add both net child migration rates, female population change, and recent-mover share	-10.016^{***}	-8.664^{***}	-6.255^{**}
	(1.799)	(3.093)	(2.841)
Panel B: Sorting measures as outcomes			
Net child migration rate (5–9 as of 2020)	-3.317^{***}	-5.864^{***}	-4.469^{**}
	(0.934)	(1.933)	(1.875)
Net child migration rate (10–14 as of 2020)	-1.171^{**}	-1.517	-0.675
	(0.547)	(1.434)	(1.406)
Female population change (100 times log change)	0.039	-1.942^{**}	-2.098^{**}
	(0.454)	(0.885)	(0.855)
Female recent-mover share	1.733^{***}	0.646^{*}	-0.240
	(0.235)	(0.392)	(0.367)
Nearest-facility fixed effects	Yes	Yes	Yes
Parent-500 m mesh fixed effects	No	Yes	Yes
Baseline controls (ten variables)	No	No	Yes
Observations	173,438	173,438	173,438

Notes: Entries compare 0–250 m with 1.25–1.50 km, using the same 173,438 cells with positive 2015 child cohorts and all four sorting measures. Panel A reports 2020 CWR differences, adds the listed controls, and weights by women ages 15–49. Panel B uses each sorting measure as the outcome. Child-migration and recent-mover coefficients are in percentage points; female population change is 100 times log growth. Child outcomes are weighted by their 2015 cohort populations; female population change by the average 2015 and 2020 counts of women ages 15–49; and recent-mover shares by women of all ages with known residence duration. Definitions are in Appendix A.7. All models exclude adult-facility cells. Standard errors in parentheses cluster by nearest facility in column (1), and by facility and parent-500 m mesh in columns (2)–(3). $^{*}p < 0.10$, $^{**}p < 0.05$, $^{***}p < 0.01$.

B.5 Residential land prices and neighborhood valuation

Table B.9 uses the predicted land price of each cell as the outcome on the same main sample, retaining the female-population weights and column conventions. A distance coefficient β_b corresponds to $100[\exp(\beta_b) - 1]$ percent higher predicted land price relative to 1.25–1.50 km. These regressions use spatially interpolated assessment prices rather than individual transactions.

Table B.9: Disability-Facility Proximity and Residential Land Prices

	(1) Facility FE	(2) Facility + 500 m FE	(3) Both FE + controls
Dependent variable: log 2020 residential land price			
0–250 m	0.0627***	0.0433***	0.0379***
	(0.0062)	(0.0042)	(0.0042)
250–500 m	0.0532***	0.0381***	0.0333***
	(0.0061)	(0.0041)	(0.0040)
500–750 m	0.0366***	0.0290***	0.0255***
	(0.0060)	(0.0038)	(0.0038)
750–1,000 m	0.0172***	0.0160***	0.0138***
	(0.0057)	(0.0035)	(0.0034)
1,000–1,250 m	0.0069	0.0083***	0.0071***
	(0.0042)	(0.0025)	(0.0024)
Baseline controls	No	No	Yes
Observations	190,747	190,747	190,747

Notes: The outcome is predicted log residential land price in 2020, based on nearby assessment points rather than individual transactions (Appendix A.8). Coefficients compare each distance band with 1.25–1.50 km. The three specifications follow Table 1, using the same 190,747 cells, excluding adult-facility cells, and weighting by women ages 15–49. Standard errors in parentheses cluster by nearest facility in column (1), and by facility and parent-500 m mesh in columns (2)–(3). $^{*}p < 0.10$, $^{**}p < 0.05$, $^{***}p < 0.01$.

B.6 Recorded crime as an alternative mechanism

B.6.1 Nationwide recorded theft

Table B.10 uses the 2020 rate for all seven theft methods as the outcome, with population weights and the three main specifications. The common sample contains 185,995 cells with at least 50 residents, after recursively removing singleton groups for facility and parent-500 m fixed effects. Appendix A.9 defines the geographic assignment and common 2020 population denominator.

Panel C of Table 2 adds this theft rate to the CWR regressions. Comparisons with and without theft use exactly the same cells and women ages 15–49 weights. The theft coefficient measures the conditional CWR difference per additional recorded theft per 1,000 residents.

Table B.10: Nationwide Theft

Distance band (km)	(1)	(2)	(3)
0–0.25	0.339***	−0.089	0.037
	(0.074)	(0.173)	(0.171)
0.25–0.50	0.097	−0.249	−0.152
	(0.064)	(0.166)	(0.164)
0.50–0.75	0.044	−0.236	−0.168
	(0.065)	(0.155)	(0.153)
0.75–1.00	−0.040	−0.305*	−0.265*
	(0.065)	(0.158)	(0.156)
1.00–1.25	0.057	−0.082	−0.076
	(0.068)	(0.102)	(0.101)
1.25–1.50 (reference)	0	0	0
Nearest-facility fixed effects	Yes	Yes	Yes
Parent-500 m fixed effects	No	Yes	Yes
Baseline controls (ten variables)	No	No	Yes
Observations	185,995	185,995	185,995

Notes: The outcome is recorded theft in 2020 per 1,000 residents, covering the seven methods in Appendix A.9. Records must report a neighborhood. Coefficients compare each band with 1.25–1.50 km. All columns use the same cells with at least 50 residents, exclude adult-facility cells, and weight by population. Specifications follow Table 1. Standard errors in parentheses cluster by nearest facility in column (1), and by facility and parent-500 m mesh in columns (2)–(3). Panel C of Table 2 instead uses theft as a CWR control and weights by women ages 15–49. $^{*}p < 0.10$, $^{**}p < 0.05$, $^{***}p < 0.01$.

Table B.11 applies the column-(3) theft-outcome specification and population weights to the alternative years and theft groupings. The corresponding all-methods 2020 estimates appear in column (3) of Table B.10.

Table B.11: Nationwide Geocoded Theft Outcomes

Panel A. All seven theft methods across years

Distance band	2020	2019	2019–2020 mean
0–0.25 km	0.037	0.183	0.110
	(0.171)	(0.226)	(0.189)
0.25–0.50 km	−0.152	−0.057	−0.104
	(0.164)	(0.214)	(0.180)
0.50–0.75 km	−0.168	−0.087	−0.127
	(0.153)	(0.197)	(0.167)
0.75–1.00 km	−0.265*	−0.179	−0.222
	(0.156)	(0.195)	(0.169)
1.00–1.25 km	−0.076	0.009	−0.034
	(0.101)	(0.124)	(0.106)
1.25–1.50 km (reference)	0	0	0

Panel B. Theft groupings, 2020

Distance band	Bicycle theft	Vehicle-related theft
0–0.25 km	0.095	−0.050
	(0.130)	(0.067)
0.25–0.50 km	−0.073	−0.067
	(0.124)	(0.064)
0.50–0.75 km	−0.059	−0.099
	(0.116)	(0.062)
0.75–1.00 km	−0.130	−0.120**
	(0.120)	(0.057)
1.00–1.25 km	−0.005	−0.060
	(0.080)	(0.039)
1.25–1.50 km (reference)	0	0

Notes: Outcomes are theft records per 1,000 residents, using 2020 population for every year. Panel A covers all seven theft methods; Panel B separates the two listed groups. Records must report a neighborhood (Appendix A.9). Coefficients compare each band with 1.25–1.50 km. All columns use the same 185,995 cells with at least 50 residents, exclude adult-facility cells, and weight by population. Models include nearest-facility and parent-500 m fixed effects and the ten baseline controls. Standard errors in parentheses cluster by facility and parent-500 m mesh. $^{*}p < 0.10$, $^{**}p < 0.05$, $^{***}p < 0.01$.

B.6.2 Tokyo town/chome crime

The Tokyo analysis uses one observation per town/chome and outcomes in incidents per 1,000 residents; source matching is described in Appendix A.9. Eligible areas have at least 50 residents and a representative point less than 1.5 km from an admissible adult disability facility. Facility-containing town/chomes are excluded, with no upper area limit. Controls are log population density, log area, and the three zoning indicators. Regressions use population weights and cluster by the included fixed-effect units.

Table B.12 estimates the five-band profile with nearest-facility and parent-1 km mesh fixed effects. Recursive singleton removal leaves 841 of the 2,250 eligible town/chomes, including seven in the 1.25–1.50 km reference band. Joint nearest-facility and parent-500 m fixed effects are rank deficient at this geographic level.

Table B.12: Tokyo Town/Chome Crime Outcomes, 2020

Distance band	All Penal Code offenses	Violent or serious offenses	Burglary	Non-burglary theft
0–250 m	−0.493	−0.679*	−0.848***	0.737
	(2.896)	(0.408)	(0.234)	(1.913)
250–500 m	−0.632	−0.801**	−0.839***	0.773
	(2.859)	(0.404)	(0.226)	(1.871)
500–750 m	−1.441	−0.828**	−0.897***	0.190
	(2.838)	(0.398)	(0.225)	(1.861)
750–1,000 m	1.112	−0.716*	−0.908***	2.183
	(2.598)	(0.386)	(0.222)	(1.706)
1,000–1,250 m	0.437	−0.816**	−0.858***	2.384
	(2.773)	(0.393)	(0.328)	(1.753)
1,250–1,500 m (reference)	0	0	0	0
Nearest-facility fixed effects	Yes	Yes	Yes	Yes
Parent-1 km mesh fixed effects	Yes	Yes	Yes	Yes
Controls	Yes	Yes	Yes	Yes
Observations	841	841	841	841

Notes: Outcomes are recorded incidents per 1,000 residents in 2020; coefficients compare each distance band with 1.25–1.50 km. The 841 town/chomes have at least 50 residents and contain no adult disability facility. Models weight by population and include nearest-facility and parent-1 km fixed effects, log population density, log area, and three zoning indicators. Standard errors in parentheses cluster by facility and parent-1 km mesh.

Only seven town/chomes remain in the reference band, so the estimates are sensitive to this small comparison group and do not establish a protective effect. Violent or serious offenses combine the two official categories. Further details are in Appendix B.6.2.

$^{*}p < 0.10$, $^{**}p < 0.05$, $^{***}p < 0.01$.

B.7 Sensitivity to unobserved confounding

Table B.13 applies the Oster (2019) proportional-selection framework to the column-(3) 0–250 m CWR coefficient. Let D be the nearest-band indicator and M the facility and parent-500 m fixed effects, ten baseline controls, and four other distance indicators. Each exercise adds one benchmark G to (D, M): both net child migration rates, all four sorting measures, predicted log residential land price, or recorded theft.

Sorting uses 173,438 cells; land price uses the 190,747-cell main sample; and theft uses 185,995 cells with at least 50 residents and non-singleton support for both fixed effects. Each comparison fixes the cells and weights (women ages 15–49). Panel A reports coefficients and conditional explanatory power without and with G.

Calculation. After weighted residualization of CWR, D, and G on M, let R_s^2 and R_f^2 be the conditional R^2 before and after adding G. The unobserved component is assumed to add the same explanatory power as the benchmark:

$$R^2_{\max} = R_f^2 + (R_f^2 - R_s^2). \tag{B.3}$$

The parameter δ measures selection on the unobserved outcome component relative to the observed benchmark. Panel B solves the exact equation at $\delta = 1$, selecting the closest valid root that continues the observed coefficient movement toward zero. It also reports the δ yielding zero, which is not a general sign-reversal threshold when there are multiple roots (Masten and Poirier, 2026).

Table B.13: Oster Sensitivity of the CWR Coefficient to Unobserved Confounding

	Residential sorting		Land price	Recorded theft
Quantity	Both child cohorts	All four measures		
Panel A: Observed coefficients and conditional explanatory power				
Observations	173,438	173,438	190,747	185,995
CWR coefficient without benchmark G	−8.0519	−8.0519	−7.3937	−7.7508
CWR coefficient with benchmark G	−7.0020	−6.2549	−6.7441	−7.7496
Conditional R_s^2 (without G)	0.00007172	0.00007172	0.00005782	0.00006403
Conditional R_f^2 (with G)	0.01445007	0.19497992	0.00026961	0.00006662
Observed conditional R^2 gain, $R_f^2 - R_s^2$	0.01437835	0.19490820	0.00021179	0.00000259
Panel B: Oster proportional selection, equal R^2 gains				
Conditional $R^2_{\max}$	0.02882843	0.38988811	0.00048140	0.00006922
Adjusted CWR coefficient at $\delta = 1$	−5.952	−4.457	−6.095	−7.748
δ yielding a zero coefficient	6.65	3.48	8.65	239.41

Notes: The target is the 0–250 m CWR difference relative to 1.25–1.50 km in specification (3). Each column adds the listed benchmark G, holding the sample and women ages 15–49 weights fixed. Panel A shows how the coefficient and explanatory power change after adding G, accounting for the other regressors. Panel B assumes that unmeasured factors add as much explanatory power as G. The parameter δ compares selection on unmeasured factors with selection on G; $\delta = 1$ means equal selection. The solution choice and assumptions follow Appendix B.7. The value yielding zero need not mark where the coefficient changes sign. These calculations concern point estimates, not statistical significance.

B.8 Robustness checks

Table B.14 restores cells containing adult disability facilities and reports the same three specifications. It checks whether excluding the population counted in facility cells drives the main association.

Table B.14: Distance to the Nearest Disability Facility with Facility-Containing Cells Re-included

Distance band (km)	(1)	(2)	(3)
0–0.25	-7.784^{***}	-9.257^{***}	-7.819^{**}
	(1.907)	(3.379)	(3.157)
0.25–0.50	−2.330	-5.417^{*}	-6.195^{**}
	(1.879)	(3.292)	(3.077)
0.50–0.75	−0.878	-5.501^{*}	-6.343^{**}
	(1.877)	(3.183)	(2.961)
0.75–1.00	1.003	−2.845	−3.829
	(1.898)	(2.894)	(2.690)
1.00–1.25	−0.793	−2.736	−2.570
	(1.911)	(2.221)	(2.114)
1.25–1.50 (reference)	0	0	0
Facility fixed effects	Yes	Yes	Yes
Parent-500 m fixed effects	No	Yes	Yes
Baseline controls	No	No	Yes
Observations	222,769	222,769	222,769

Notes: Entries are differences in the 2020 CWR (children ages 0–4 per 1,000 women ages 15–49) relative to 1.25–1.50 km. This sample includes cells containing adult disability facilities. All columns use the same cells and weights equal to the number of women ages 15–49. Specifications and clustering follow Table 1. Standard errors are in parentheses. $^{*}p < 0.10$, $^{**}p < 0.05$, $^{***}p < 0.01$.

Table B.15 compares the standard CWR with the alternative age-20–39 denominator defined in Appendix A.10. Both use a common eligible sample, but each outcome uses its own denominator as the analytic weight.

Table B.15: Alternative CWR Denominator on Common Support

Outcome	(1)	(2)	(3)	N
CWR using women ages 15–49	-10.101^{***} (2.324)	-13.833^{***} (3.875)	-10.785^{***} (3.611)	140,679
CWR using women ages 20–39	-27.091^{***} (4.251)	-26.661^{***} (6.827)	-18.777^{***} (5.883)	140,679

Notes: Entries compare the 0–250 m and 1.25–1.50 km bands in 2020. Each CWR is children ages 0–4 per 1,000 women in the indicated age group. Both rows use the same cells, with at least 10 women ages 20–39. Each regression is weighted by the number of women in its denominator. Specifications and clustering follow Table 1. Standard errors are in parentheses. $^{*}p < 0.10$, $^{**}p < 0.05$, $^{***}p < 0.01$.

Table B.16 extends the estimation window to 2 km and adds two outer-band indicators while retaining the main 1.25–1.50 km reference band.

Table B.16: Extending the Estimation Window to 2 km with an Unchanged Reference Band

Distance band (km)	(1)	(2)	(3)
0–0.25	-5.798^{***}	-8.023^{**}	-7.484^{**}
	(1.921)	(3.427)	(3.220)
0.25–0.50	−1.781	-5.635^{*}	-6.435^{**}
	(1.846)	(3.286)	(3.089)
0.50–0.75	−0.178	-5.609^{*}	-6.478^{**}
	(1.837)	(3.174)	(2.971)
0.75–1.00	1.469	−2.870	−3.937
	(1.840)	(2.886)	(2.701)
1.00–1.25	−0.881	−2.739	−2.680
	(1.853)	(2.207)	(2.124)
1.25–1.50 (reference)	0	0	0
1.50–1.75	−1.397	−0.763	−0.108
	(1.951)	(2.497)	(2.301)
1.75–2.00	−1.868	−4.424	−3.650
	(2.714)	(3.649)	(3.448)
Facility fixed effects	Yes	Yes	Yes
Parent-500 m fixed effects	No	Yes	Yes
Baseline controls	No	No	Yes
Observations	203,696	203,696	203,696

Notes: Entries are differences in the 2020 CWR (children ages 0–4 per 1,000 women ages 15–49). The sample extends to 2 km, but the reference band remains 1.25–1.50 km. All columns use the same cells, exclude cells containing adult disability facilities, and weight by the number of women ages 15–49. Specifications and clustering follow Table 1. Standard errors are in parentheses. $^{*}p < 0.10$, $^{**}p < 0.05$, $^{***}p < 0.01$.

Table B.17 holds the coefficient estimates fixed and allows residual spatial correlation to cross facility and parent-mesh boundaries. It reports Conley-type standard errors for the three distance cutoffs discussed in Section 5.

Table B.17: Spatial-Inference Robustness

Inference	Coefficient	S.E.	p-value	N
Facility and parent-500 m clusters	-7.394^{**}	3.216	0.022	190,747
Conley, 0.5 km	-7.394^{**}	2.945	0.012	190,747
Conley, 1 km	-7.394^{**}	3.144	0.019	190,747
Conley, 2 km	-7.394^{**}	3.275	0.024	190,747

Notes: All rows report the 0–250 m CWR coefficient from column (3) of Table 1, relative to 1.25–1.50 km, using the same sample and weights based on women ages 15–49. Only standard errors change: the first row clusters by facility and parent-500 m mesh; the other rows allow spatial correlation up to the stated distance using Conley standard errors. $^{*}p < 0.10$, $^{**}p < 0.05$, $^{***}p < 0.01$.

Table B.18 estimates a Poisson pseudo-maximum likelihood (PPML) rate model. Let C_i be the number of children ages 0–4 in cell i in 2020, and let $W_i > 0$ be the number of women ages 15–49. The fully controlled regression specifies the conditional mean as

$$\mu_i \equiv \mathrm{E}[C_i \mid D_i, X_i, f(i), m(i), W_i],$$
$$\log \mu_i = \log W_i + \sum_{b=0}^{4} \beta_b D_{ib} + X_i' \gamma + \alpha_{f(i)} + \delta_{m(i)}. \tag{B.4}$$

The offset $\log W_i$ has coefficient one, so μ_i / W_i is the expected child–woman rate. The distance coefficients imply percentage differences $100[\exp(\beta_b) - 1]$ from the reference band. Fixed effects, controls, and clustering follow the three common columns.

PPML uses no additional analytic weights. Zero child counts remain unless removed by the support restrictions: all three columns use the same 190,266 cells after dropping all-zero fixed-effect groups and recursively removing singletons.

Table B.18: PPML Rate Specification

Distance band (km)	(1)	(2)	(3)
0–0.25	−0.0355***	−0.0404**	−0.0313*
	(0.0102)	(0.0176)	(0.0162)
0.25–0.50	−0.0139	−0.0287*	−0.0269*
	(0.0097)	(0.0168)	(0.0155)
0.50–0.75	−0.0052	−0.0288*	−0.0277*
	(0.0097)	(0.0163)	(0.0149)
0.75–1.00	0.0042	−0.0146	−0.0159
	(0.0097)	(0.0148)	(0.0135)
1.00–1.25	−0.0052	−0.0138	−0.0122
	(0.0098)	(0.0115)	(0.0109)
1.25–1.50 (reference)	0	0	0
0–0.25 km rate difference (%)	−3.49	−3.96	−3.08
Facility fixed effects	Yes	Yes	Yes
Parent-500 m fixed effects	No	Yes	Yes
Baseline controls	No	No	Yes
Observations	190,266	190,266	190,266

Notes: PPML models the 2020 count of children ages 0–4. The log number of women ages 15–49 enters as an offset with coefficient one; no additional weights are used. Coefficients are log differences in the child–woman rate relative to 1.25–1.50 km; percentage differences are $100[\exp(\widehat{\beta}) - 1]$. The common sample retains zero child counts, except cells dropped because their fixed-effect groups contain only zeros or a single observation. Fixed effects and controls follow Table 1. Standard errors in parentheses are clustered by nearest facility in column (1), and by facility and parent-500 m mesh in columns (2)–(3). Stars use two-sided normal tests: $^{*}p < 0.10$, $^{**}p < 0.05$, $^{***}p < 0.01$.

References for the Appendix

Amemiya, Mamoru and Daisuke Tanaka, "Database of Geocoded Theft Records at the Neighborhood Level in Japan: 2020 Edition," University of Tsukuba, Division of Policy and Planning Sciences Commons Data Bank; CC BY 4.0, 2022, URL: https://commons.sk.tsukuba.ac.jp/data (visited on 08/30/2026).

Amemiya, Mamoru and Mayuko Yamane, "Database of Geocoded Theft Records at the Neighborhood Level in Japan: 2019 Edition," University of Tsukuba, Division of Policy and Planning Sciences Commons Data Bank; CC BY 4.0, 2021, URL: https://commons.sk.tsukuba.ac.jp/data (visited on 08/30/2026).

GraphHopper, "GraphHopper Routing Engine," version 11.0, 2026, URL: https://github.com/graphhopper/graphhopper (visited on 09/02/2026).

Masten, Matthew A. and Alexandre Poirier, "The Effect of Omitted Variables on the Sign of Regression Coefficients," *American Economic Review*, 2026, *116* (7), 2685–2710, DOI: 10.1257/aer.20230242.

Ministry of Land, Infrastructure, Transport and Tourism, "National Land Numerical Information: Welfare Facilities Data (P14), 2011 Edition," Product specification version 1.3; P14-11 prefectural archives; coordinates in JGD2000, 2011, URL: https://nlftp.mlit.go.jp/ksj/gml/datalist/KsjTmplt-P14.html (visited on 09/10/2026).

Ministry of Land, Infrastructure, Transport and Tourism, "National Land Numerical Information: Welfare Facilities Data (P14), 2015 Edition," Reference date: September 30, 2015; product specification version 1.3; P14-15 prefectural archives, 2015, URL: https://nlftp.mlit.go.jp/ksj/gml/datalist/KsjTmplt-P14-2015.html (visited on 09/06/2026).

Ministry of Land, Infrastructure, Transport and Tourism, "National Land Numerical Information: Land Use Zoning Data (A29), 2019 Edition," 2019, URL: https://nlftp.mlit.go.jp/ksj/gml/datalist/KsjTmplt-A29-2019.html (visited on 08/28/2026).

Ministry of Land, Infrastructure, Transport and Tourism, "National Land Numerical Information: Land Price Publication Data (L01), 2020 Edition," Valuation date: January 1, 2020; national archive L01-20_GML.zip, 2020a, URL: https://nlftp.mlit.go.jp/ksj/gml/datalist/KsjTmplt-L01-v2_5.html (visited on 09/06/2026).

Ministry of Land, Infrastructure, Transport and Tourism, "National Land Numerical Information: Prefectural Land Price Survey Data (L02), 2020 Edition," Valuation date: July 1, 2020; national archive L02-20_GML.zip, 2020b, URL: https://nlftp.mlit.go.jp/ksj/gml/datalist/KsjTmplt-L02-2020.html (visited on 09/06/2026).

Ministry of Land, Infrastructure, Transport and Tourism, "National Land Numerical Information: Railway Data (N02), 2020 Edition," 2020c, URL: https://nlftp.mlit.go.jp/ksj/gml/datalist/KsjTmplt-N02-v2_3.html (visited on 08/29/2026).

Ministry of Land, Infrastructure, Transport and Tourism, "National Land Numerical Information: Welfare Facilities Data (P14), 2021 Edition," 2021, URL: https://nlftp.mlit.go.jp/ksj/gml/datalist/KsjTmplt-P14-2021.html (visited on 09/04/2026).

Ministry of Land, Infrastructure, Transport and Tourism, "National Land Numerical Information: Bus Stop Data (P11), 2022 Edition," 2022, URL: https://nlftp.mlit.go.jp/ksj/gml/datalist/KsjTmplt-P11-v3_0.html (visited on 08/29/2026).

OpenStreetMap contributors, "OpenStreetMap: Historical Japan Extract, January 1, 2021," Regional extracts distributed by Geofabrik GmbH, 2021, URL: https://download.geofabrik.de/asia/japan.html (visited on 09/02/2026).

Oster, Emily, "Unobservable Selection and Coefficient Stability: Theory and Evidence," *Journal of Business & Economic Statistics*, 2019, *37* (2), 187–204, DOI: 10.1080/07350015.2016.1227711.

Statistics Bureau of Japan, "2015 Population Census Regional Mesh Statistics: Data Definition T001178 (Population by Sex and Five-Year Age Group)," 2015a, URL: https://www.e-stat.go.jp/help/data-definition-information/downloaddata/T001178.pdf (visited on 08/29/2026).

Statistics Bureau of Japan, "2015 Population Census Regional Mesh Statistics: Data Definition T001207 (Housing Tenure and Building Form)," 2015b, URL: https://www.e-stat.go.jp/help/data-definition-information/downloaddata/T001207.pdf (visited on 08/31/2026).

Statistics Bureau of Japan, "2020 Population Census Regional Mesh Statistics: Data Definition T001175 (Population by Sex and Five-Year Age Group, JGD2000)," 2020a, URL: https://www.e-stat.go.jp/help/data-definition-information/downloaddata/T001175.pdf (visited on 08/29/2026).

Statistics Bureau of Japan, "2020 Population Census Regional Mesh Statistics: Data Definition T001186 (Housing Tenure and Building Form)," 2020b, URL: https://www.e-stat.go.jp/help/data-definition-information/downloaddata/T001186.pdf (visited on 08/31/2026).

Statistics Bureau of Japan, "2020 Population Census: Instructions for Completing the Questionnaire," 2020c, URL: https://www.stat.go.jp/data/kokusei/2020/pdf/kinyu.pdf (visited on 09/03/2026).

Statistics Bureau of Japan, "2020 Population Census: Small-Area Boundary Data and Statistics," 2020d, URL: https://www.e-stat.go.jp/gis/statmap-search?aggregateUnitForBoundary=A&page=1&type=2 (visited on 08/30/2026).

Statistics Bureau of Japan, "2020 Population Census Regional Mesh Statistics: Data Definition T001109 (Employment, Education and Migration)," 2022a, URL: https://www.e-stat.go.jp/help/data-definition-information/downloaddata/T001109.pdf (visited on 08/28/2026).

Statistics Bureau of Japan, "2020 Population Census Regional Mesh Statistics: Data Definition T001187 (Previous Residence and Place of Work or School)," 2022b, URL: https://www.e-stat.go.jp/help/data-definition-information/downloaddata/T001187.pdf (visited on 09/03/2026).

Statistics Bureau of Japan, "2020 Population Census Regional Mesh Statistics: Data Definition T001196 (Population by Sex and Five-Year Age Group)," 2025, URL: https://www.e-stat.go.jp/help/data-definition-information/downloaddata/T001196.pdf (visited on 08/28/2026).

Statistics Bureau of Japan, "Regional Mesh Statistics," 2026, URL: https://www.stat.go.jp/data/mesh/m_tuite.html (visited on 09/04/2026).

Tokyo Metropolitan Police Department, "Recorded Offenses by Municipality, Town/Chome, Offense Type, and Method," 2026, URL: https://www.keishicho.metro.tokyo.lg.jp/about_mpd/jokyo_tokei/jokyo/ninchikensu.html (visited on 08/30/2026).